PERGAMON

Deep-Sea Research II 49 (2002) 1481–1511

DEEP-SEA RESEARCH
PART II

www.elsevier.com/locate/dsr2

Volume transport and property distributions of the Mozambique Channel

Steven F. DiMarco[a,*], Piers Chapman[a], Worth D. Nowlin Jr.[a], Peter Hacker[b], Kathleen Donohue[c], Mark Luther[d], Gregory C. Johnson[e], John Toole[f]

[a] *Department of Oceanography, Texas A&M University, College Station, TX 77843-3146, USA*
[b] *School of Ocean and Earth Science and Technology, University of Hawaii, Honolulu, HI, 96822, USA*
[c] *Graduate School of Oceanography, University of Rhode Island, Narragansett, RI 02882, USA*
[d] *Department of Marine Science, University of South Florida, St. Petersburg, FL 33701, USA*
[e] *NOAA/PMEL, Seattle, WA, USA*
[f] *Woods Hole Oceanographic Institution, Woods Hole, MA 02543, USA*

Accepted 26 September 2001

Abstract

We summarize previous estimates of volume transport and property distributions through the Mozambique Channel and offer additional estimates and measurements based on recently acquired hydrographic and float data. Previously published property distributions are consistent with southward spreading through the Channel. Waters of the Mozambique Channel are characterized by shallow and intermediate oxygen minima separated by a relative maximum. Based on hydrographic sections, the intermediate maximum in dissolved oxygen is seen to decrease in value as it spreads southward. The highest values are found in the westward flow of the South Equatorial Current just north of Madagascar and within the western 200 km of the Channel. Similarly, oxygen concentrations at the intermediate oxygen minimum, which derives from the Arabian Sea, increase southwards, while its depth increases from 900 to 1100 m, supporting previous studies and indicating southward spreading and mixing along the Mozambique Channel. Historical transports based on hydrographic data in the Channel vary from 5 Sv northward to 26 Sv southward depending on reference level and time of the year. Balancing transport below 2500 m (the sill depth in the Channel), we estimate the net southward transports above this depth to be 29.1 and 5.9 Sv for the northern and southern sections, respectively—the difference is presumably related to seasonality and eddy variability superimposed on the mean flow. Individual deep float trajectories show the presence of many eddies, but the overall flow in the channel is southward, and broadly consistent with hydrography. Model outputs also show mean southward transport with considerable seasonal variability. Satellite data show high variability in sea surface height anomalies and high eddy kinetic energy associated with eddy activity. Although the geostrophic transport values are consistent with the historical limits, the lowered ADCP measurements suggest a substantial barotropic component to the flow. Direct long-term measurements of the current are needed to quantify its magnitude and variability. © 2002 Published by Elsevier Science Ltd.

*Corresponding author. Tel.: +1-979-862-4168; fax: +1-979-847-8879.
E-mail address: sdimarco@tamu.edu (S.F. DiMarco).

0967-0645/02/$ - see front matter © 2002 Published by Elsevier Science Ltd.
PII: S0967-0645(01)00159-X

1. Introduction

Despite the obvious importance of the Mozambique Channel, which separates the island of Madagascar from the rest of Africa (Fig. 1), as a commercial transport route between the Cape of Good Hope and the northern Indian Ocean, prior literature and observations yield no firm conclusions regarding the characteristics of the through-channel transport. There is a general assumption that flow through the Channel supplies part of the flow of the strong Agulhas Current further south (e.g., Gordon, 1986), but the few previous studies suggest considerable interannual variability (e.g., Lutjeharms, 1972; Saetre and Jorge da Silva, 1984). MacDonald (1998) finding no significant net flow through the channel, wrote: "Given the range in previous estimates and the variability

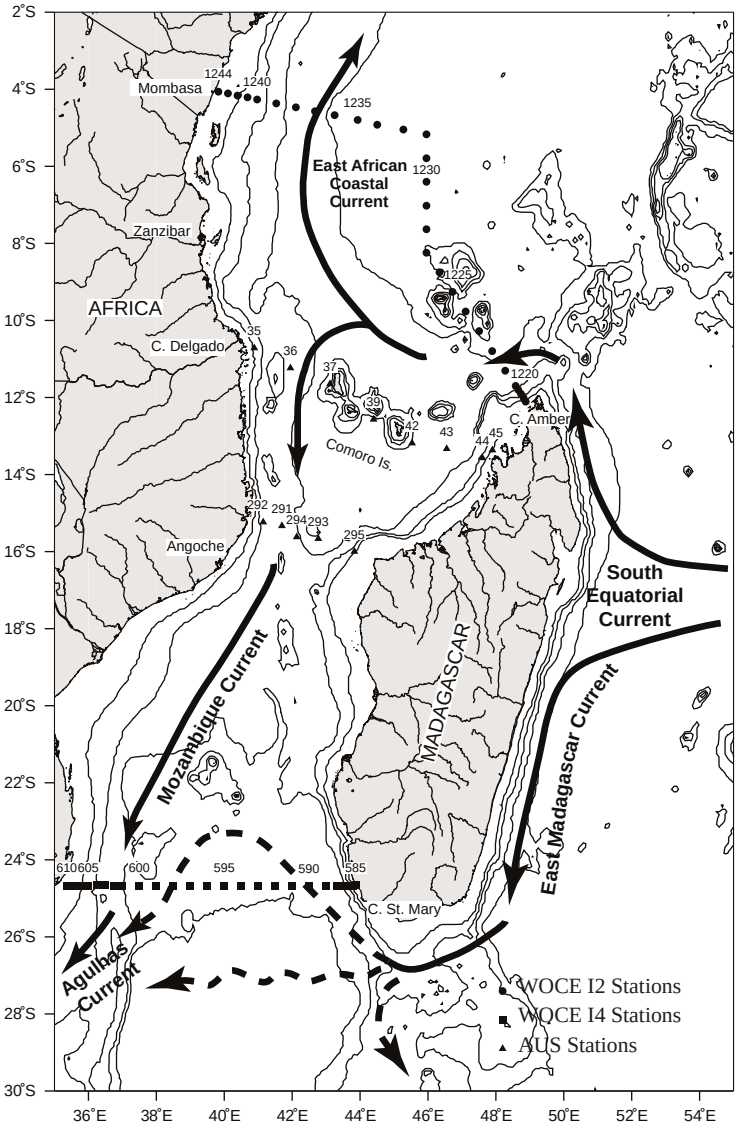

Fig. 1. Bathymetry of the Mozambique Channel region showing positions of stations from which hydrographic data are presented. Regional current regimes are shown schematically.

suggested by the Semtner and Chervin model and our own lack of resolution, almost any result in this region would have to be deemed acceptable." The Indian Ocean, especially at the western boundary plays an important part in the global redistribution of mass, heat, freshwater and other properties. Here, we report further information on flow through the channel.

As early as 1935, Clowes and Deacon presented salinity and oxygen profiles along a meridional section through the Mozambique Channel and inferred southward flow of North Indian Ocean Deep Water through the Channel (Fig. 2). The upper bound of this water is characterized by an oxygen minimum centered near 1000 m that deepens as it moves southward through the Channel. These authors also suggested large variations in salinity and volume flow through the Mozambique Channel would be found, and suggested these were probably related to salinity changes in the coastal current, monsoonal winds, and variability in the South Equatorial Current (SEC).

We report here new hydrographic measurements, selected property distributions, direct velocity observations, and transport estimates obtained during cruises of the World Ocean Circulation Experiment (WOCE) in 1995 and 1996 at the southern and northern ends of the channel, respectively. The transport estimates are compared to model results that suggest a southward flow with large seasonal variability through the channel, as well as to Lagrangian trajectories and satellite observations in the vicinity of the channel.

2. Data

To examine the continuity of properties and geostrophic transport estimates through the Mozambique Channel, we used three hydrographic data sets: two from the WOCE Hydrographic Program (WHP) lines I2 and I4 and one from a 1965 Australian cruise across the Mozambique Channel at 12°S and 15°S. (The 1965 data were obtained from the US National Oceanographic Data Center.) WOCE Stations 1216–1244 were collected as part of WHP I2 aboard R/V *Knorr* during 14–21 January 1996 north of the Mozambique Channel from the northern tip of Madagascar near Cape Amber to the African coast at Mombasa, Kenya. The I2 section (Fig. 1) includes three segments. The eastern two segments from Cape Amber to 5.2°S (station 1232) form a mostly north-south section, while the western segment between 46°E and the coast of Africa is aligned almost east-west. Stations 585–610 from the southern tip of Madagascar to Africa were collected as part of WHP leg I4 aboard R/V *Knorr* during 15–19 June 1994. The Australian stations at about 12°S (stations 35–45) and 15°S (stations 291–295) were occupied in May 1965. Stations 291–295 are situated just north of the Davie Ridge, which defines the saddle in the narrowest part of the Mozambique Channel. All station locations are shown in Fig. 1. The WOCE hydrographic stations were generally spaced 55 km apart, with closer spacing near the continental slope to sample adequately smaller scale currents associated with steep topography. At each station a rosette equipped with a CTD was lowered to the bottom. The CTD was calibrated prior to and following the cruise as recommended by SCOR Working Group 51 (Unesco, 1988; Müller et al., 1994). Water samples were collected at a maximum of 36 depths distributed throughout the water column. These were sub-sampled for shipboard analysis of salinity oxygen, nutrients and other parameters. All chemical analyses were conducted using recommended WOCE methods (WOCE, 1994).

Although use of data that are widely separated in time in such a variable region is not ideal, the two Australian lines are the only ones that contain sections of oxygen taken across the narrow portion of the Mozambique Channel. We use them in this case to show that there is a general trend in water properties through the channel. Although the stations sampled to the bottom, the station spacing is too broad to use the data to estimate the transport.

Shipboard and lowered acoustic Doppler current profiler (LADCP) measurements were made along WOCE lines I2 and I4. A 4-antennae Ashtech receiver provided heading corrections on both lines. The following briefly describes the

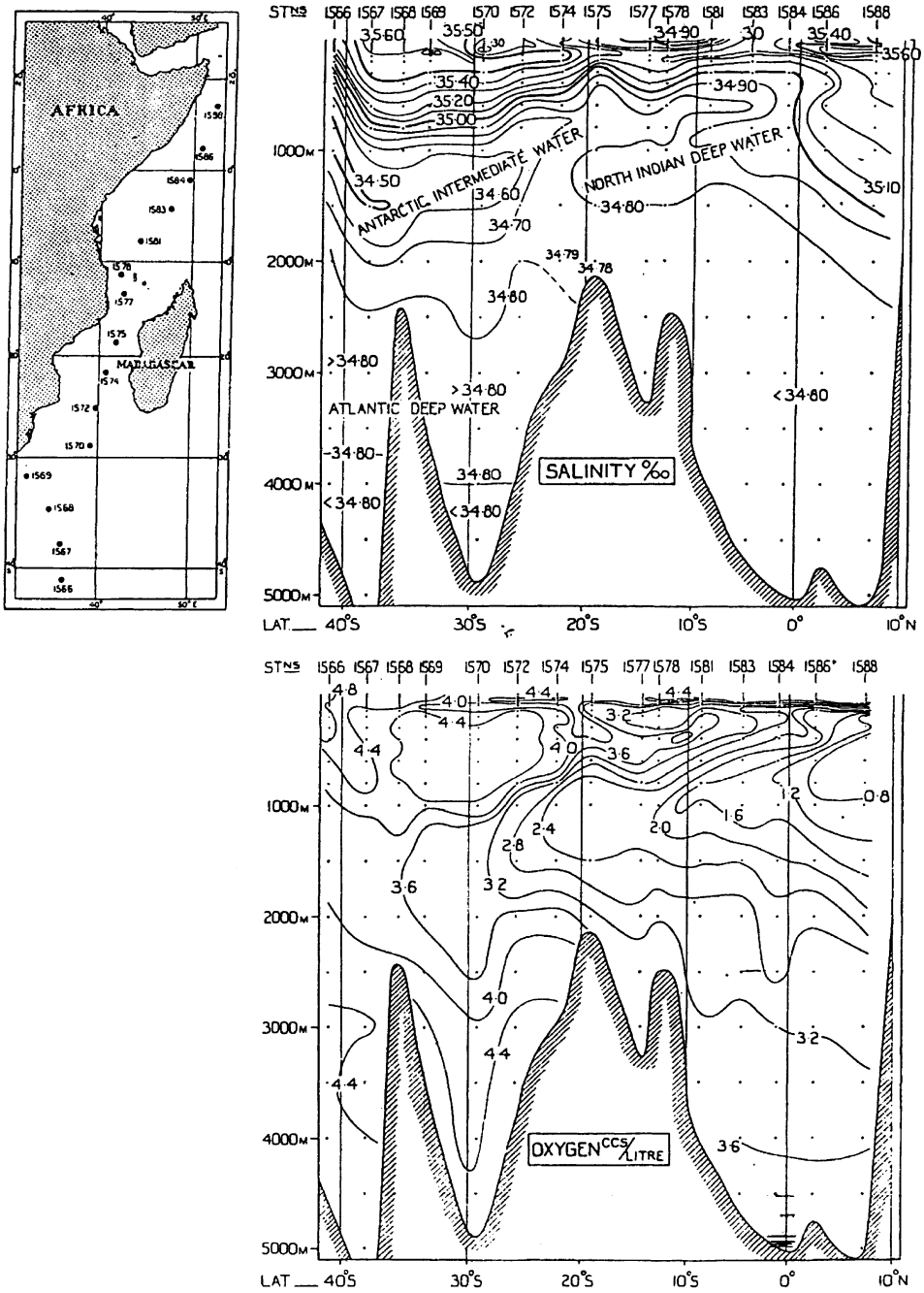

Fig. 2. Vertical sections of salinity and oxygen along a section through the Mozambique Channel. (Reprinted by permission from Nature, 136, pp. 936–938, MacMillan Magazines Ltd., copyright 1935.)

accuracy of the two systems, since the LADCP transport calculations depend greatly on any biases. Data from the shipboard system (not shown) were used to identify any large bias in the LADCP data. On I2 a failed beam in the shipboard system limited velocity observations to a depth of 250 m; on I4 the depth-range extended to 350–400 m. Errors in the shipboard system are $<0.01\,m\,s^{-1}$ for I2, with P-code GPS navigation and $0.02\,m\,s^{-1}$ for I4, with standard P/Y-code navigation for 2-h averages.

Vertical profiles of horizontal velocity were obtained at each station (except #610 on I4) using an LADCP mounted on the CTD/rosette system. The LADCP was a 153-kHz broadband unit (RD Instruments, model BBCS 150). Fisher and Visbeck (1993), Send (1994) and Hacker et al. (1996) provide details on data processing, accuracy, and error estimation. We estimate an rms error for the LADCP data in the range ± 0.03–$0.05\,m\,s^{-1}$ below 1000 m and somewhat larger above 1000 m depending on internal wave activity. For the depth-averaged component at each station we estimate measurement errors at <0.01–$0.02\,m\,s^{-1}$ (depending on station depth) with possible biases (unknown) of $0.01\,m\,s^{-1}$ (Hacker et al., 1996). Barotropic tidal currents are a potential source of noise; these were removed at each station using estimates from altimeter data and the TPXO.3 global tidal model (Dushaw et al., 1997; Egbert et al., 1994). For the I2 line, these tidal corrections were as large as $0.10\,m\,s^{-1}$ for the four stations near Cape Amber, and $<0.04\,m\,s^{-1}$ for the rest of the section. Along I4 the corrections were largest, $0.07\,m\,s^{-1}$ near 42.5°E, with corrections $<0.04\,m\,s^{-1}$ west of 40°E.

Although a somewhat noisy calculation, comparisons between the shipboard and LADCP observations during CTD stations suggest a possible LADCP bias to the south/west (cross-track) along I2 ($0.005\,m\,s^{-1}$) and to the north along I4 ($0.017\,m\,s^{-1}$). If true, such biases can introduce substantial error in transport estimates when integrated across an entire line; for a 2500-m deep section, the error is between 1.2 and 4.2 Sv per 100 km.

During WOCE, 213 Autonomous Lagrangian Current Explorer (ALACE) floats (Davis et al., 1992) were launched in the Indian Ocean at a nominal depth of 1000 m. The floats remained at their predetermined "parking" depth for a set period (25 days), then returned to the surface and broadcast their position via satellite. They then returned to 1000 m for another 25 days. Each float is capable of as many as 75–100 cycles, resulting in a series of velocity measurements that can be considered independent. We have used the data (courtesy of R. Davis) from floats which entered our study region to help us explain flows at mid-depth. During their life, the floats have a tendency to rise in the water column; most of the data discussed in this paper are from 800 to 950 m depth.

3. Historical background and interpretations

3.1. General circulation patterns and current measurements

The large-scale upper layer current regime in the region is complex (Fig. 1). The SEC is driven mainly by the local wind stress and the flow of the interior Subtropical gyre, but there is also a smaller contribution from the Indonesian throughflow (Gordon and McClean, 1999). The SEC flows westward across the Indian Ocean and bifurcates at the east coast of Madagascar near 20°S (Swallow et al., 1988; Hellerman and Rosenstein, 1983). The southward flowing branch is known as the East Madagascar Current (EMC), while the northern limb turns west on reaching Cape Amber, the northern tip of the island. During the southwest monsoon (May–September), part of the northern branch (the Zanzibar or East African Coastal Current) continues north to feed the northward-flowing Somali Current; however, during the northeast monsoon (November–February), its flow appears to extend northward only to about 3°S before turning eastward and contributing to the eastward flowing Equatorial Countercurrent (Swallow et al., 1988). The remainder of the northern branch of the SEC passing Madagascar turns southward near the African coast and becomes the Mozambique Current (MC), which flows south through the Mozambique Channel

(Tomczak and Godfrey, 1994) apparently year-round. A major question, however, is whether the flow through the Mozambique Channel is continuous or discontinuous.

Mariners have long been aware of the surface flows in the region. According to ships' drift records (Duncan and Schladow, 1981; Saetre, 1985; Lutjeharms et al., 2000), speeds along the western edge of the Mozambique Channel are considerably higher than elsewhere in the region; the mean appears to be near 1.0–1.5 m s^{-1}, with maxima >2 m s^{-1}. This high-speed region extends from north of the Comoro islands (12°S), through the narrowest part of the Channel, and down the coast of Africa until it merges into the Agulhas Current near 24°S. Outside the channel, the EMC similarly shows a continuous band where velocities exceed 1 m s^{-1}. This extends from Cape Amber in the north past Cape St. Mary at the southern tip of the island and across to Africa. A few isolated records have velocities >1.5 m s^{-1}; these are concentrated at Cape Amber and in the southern portion of the EMC. Even the band of velocity >1.0 m s^{-1} is not continuous in either space or time, however, and Lutjeharms et al. (2000) suggest that mean speeds in the EMC can vary considerably, between 20 and 90 cm s^{-1}.

There are apparently regions within the Mozambique Channel where velocities increase. Duncan and Schladow (1981) claimed that the highest speeds (>1.5 m s^{-1}) were concentrated either north of 20°S or south of 30°S. Saetre (1985), however, found maxima in three regions (12–16°S, 21–25°S, and 27–29°S), while Lutjeharms et al. (2000) suggested 12–16°S and south of 23°S as regions of fastest southward flow. Saetre claimed that the strongest currents were found in summer (November–April), but Lutjeharms et al. (2000) disputed this and stated that they occur in winter and spring (June–November)! These authors disagree also on surface flow in the EMC. Saetre found no temporal variability (in agreement with the subsurface current meter data of Schott et al., 1988), while Lutjeharms et al. suggested a seasonal cycle with maximum southward velocities in winter and spring, in phase with the prevailing wind and the flow of he SEC.

Direct measurements from surface drifters add little to our knowledge of this region. Molinari et al. (1990) analyzed the tracks of 142 surface drifters deployed between 1975 and 1987 in the tropical Indian Ocean, but very few entered the Channel. Almost all drifters passing north of Cape Amber continued westward between 10°S and 12°S towards the African coast. The few drifters that ended up in the channel experienced considerable eddy variability. A later analysis (Shenoi et al., 1999) updated the data set to 1998, but again found little sign of a preferred flow direction within the Channel south of about 12°S. East of Madagascar, the surface flow in the SEC approaching the island near 20°S, either moved rapidly south in the EMC or northwards along the eastern side of the island. This north movement agrees with ship drift observations reported by Lutjeharms et al. (2000).

The EMC flows south along the east coast of Madagascar as a western boundary current (Schott et al., 1988), and appears to round the southern end of the island as a westward-flowing stream. The acceleration of this narrow current along the steep continental slope induces upwelling inshore, particularly at the southern end of the island where the shelf widens (Di Marco et al., 2000; Lutjeharms and Machu, 2000). At this point several flow pathways are realized (Tomczak and Godfrey, 1994). At times, part of the flow may turn north to enter the Mozambique Channel then perform a counterclockwise loop to continue south along the coast of Africa. Tchernia (1980) pictured this flow continuing up the west coast of Madagascar as the West Madagascar Current before turning counterclockwise near the northern end of the island to join the southward flowing MC (which he estimated at 20 Sv). Hydrographic (Gründlingh, 1993) and surface drifter data (Shenoi et al., 1999) support this pattern, although the northward loop is often displaced to the west away from the Madagascan coast, with sea-surface temperature images frequently showing very warm water pushing south along the west coast of the island (Di Marco et al., 2000).

There are two other possible routes for water rounding the southern end of Madagascar. The first is for it to separate from the coast near C. St.

Mary, flow due west across the Mozambique Basin towards the African shelf and then turn south to contribute to the Agulhas Current (Gründlingh, 1985a, 1987, 1993; Lutjeharms, 1988a). A final possibility is that the waters of the EMC never reach the African coast but retroflect in the vicinity of the Madagascar Ridge south of the island. Both Lutjeharms (1988b) and Di Marco et al. (2000) show SST images suggesting a retroflection there.

While the evidence for all three possible flow patterns remains contradictory on short time scales, seasonal averaging, based on satellite altimetry, suggests that the first two possibilities are more likely. Heywood and Somayajulu (1997) have shown that the westward extension of the EMC and its associated eddy field is strongest in austral winter and weakest in summer. In winter, the flow appears to cross the Mozambique Basin directly, but in summer the current often loops northward along the west coast of Madagascar. The seasonal change in eddy kinetic energy (EKE), both east of Madagascar and in the Mozambique Channel, agrees with changes in the local wind-stress field, which varies depending on the season of the monsoon. EKE during the monsoons themselves is also greater than during the inter-monsoon periods (Lutjeharms et al., 2000). Heywood and Somayajulu noted, however, that the EKE in the Mozambique Current at $>0.2\,m^2\,s^{-2}$ was always greater than that of the EMC ($0.08–0.12\,m^2\,s^{-2}$).

From a combination of direct current measurements and hydrography, Swallow et al. (1988) and Schott et al. (1988) found no detectable seasonal signal below 200 m in either branch of the SEC; they estimated the transport of the northern branch north of Madagascar to be about 30 Sv northwestward ($1\,Sv = 1 \times 10^6\,m^3\,s^{-1}$) and the transport of the southern branch at 23°S east of Madagascar to be about 21 Sv southward.

Although the region between Madagascar and the African coast contains many eddies, these are apparently not caused by shedding at the EMC retroflection. Some have been shown to originate at the Mozambique Ridge, possibly related to the conservation of potential vorticity as the current moves into deeper water (Gründlingh, 1985a, 1989). In many cases the presence of the ridge generates a pair of eddies, one cyclonic and one anticyclonic (Gründlingh, 1989), and several eddies of either sign may be present simultaneously (Gründlingh et al., 1991). Very recent data (De Ruijter et al., 2002) also suggest that eddies are formed further north within the Mozambique Channel itself at the rate of about four per year, probably triggered by Rossby waves originating in the eastern Indian Ocean.

Within the Mozambique Channel, data analysis is complicated by the fact that many cruises did not sample across its whole width, but only on the Mozambican side. Moreover there are few reliable oxygen or nutrient data from the region, and almost none of the historic stations sampled to the bottom. The best hydrographic coverage of the region is that of Menaché (1963), who published a map of dynamic topography inside the Mozambique Channel based on 65 hydrographic stations (11 cross-channel lines and 1 along-channel line) from the Comoro Islands to 30°S during the austral spring of 1957 (prior to the northeast monsoon). Only five of these stations extend below 1200 m (none below 1500 m), and only temperature and salinity were sampled. Menaché concluded that the surface circulation (relative to 1000 db) was closed in the southern part of the channel where the strong southward flow of the MC turned eastward at about 24°S and then flowed northward along the west coast of Madagascar. Later, Zahn (1984) re-examined portions of the data used by Menaché and concluded that the throughflow of the MC was 6 Sv, with transports in the western part of a section near 15°S of almost 21 Sv. Zahn also estimated northward transport of 5 Sv relative to 1000 m across a zonal line at 26°S in the southern part of the channel. The transports quoted by Zahn, however, may be an underestimate (Tomczak and Godfrey, 1994) because of the known western intensification of the flow and the poor sampling of key areas adjacent to the African and Madagascar continental shelves, particularly on the southern line. More recently, Nehring et al. (1984) and Donguy and Piton (1991) showed that, in the upper 500–600 m at least, there is considerable southward flow in the Channel.

Gründlingh (1993) summarized previous descriptions of the flow in the Mozambique Channel by saying: "Inside the Mozambique Channel the flow is more confused [than at the entrances] and the variability greater, as the southward moving water mixes with water entering from the south in a series of interwoven eddies." However, Gründlingh (1985b, 1993) concluded that net southward flow through the Mozambique Channel contributed to the Agulhas Current. Harris (1972) concurred, stating that it was one of four main sources of the Agulhas Current and contributed approximately 10 Sv of the estimated 72 Sv in that current. The recent data of De Ruijter et al. (2002) conform to the idea of Mozambique Channel water contributing to the Agulhas Current, but these authors suggest that the flow is discontinuous and consists of "a regular train of poleward propagating… eddies". In summary, the overall impression from the historical literature is of a very variable region, but a generally southward net flow.

3.2. Water properties

Water properties also support the hypothesis of net southward flow through the Mozambique Channel, as first discussed by Clowes and Deacon (1935). The intermediate oxygen minimum, with values $<20\,\mu mol\,kg^{-1}$, originates at depths near 400–600 m in the Arabian Sea; the intermediate salinity maximum in the western Indian Ocean originates in the Red Sea (Wyrtki, 1971). As these waters spread southward the oxygen minimum and salinity maximum erode and deepen. The oxygen minimum provides particularly clear evidence of its northern origin, contrasting with the higher values found above and below it in the Subantarctic Mode Water and North Atlantic Deep Water, both originating from the south.

This idea of southward spreading is corroborated in Wyrtki's (1971) atlas of hydrographic data from the Indian Ocean. Maps of properties on intermediate isopycnals (plates 244–254) and the core of the Red Sea Water (plates 282–285), the oxygen maximum (plates 308–314), and the deep oxygen minimum (plates 316–322) show net southward spreading of water through the Mozambique Channel. The northern influence is most pronounced along the western side of the Channel, but considerably stronger on the eastern side of the Channel than at the same latitudes east of Madagascar. The frequent occurrence of low-oxygen, high-salinity water of Red Sea origin further south in the Agulhas Current (e.g., Gordon, 1986; Gordon et al., 1987; Beal et al., 2000) confirms Wyrtki's analysis.

The WOCE data provide a consistent picture. For example, Fig. 3 shows potential temperature vs. salinity from CTD stations west and east of Madagascar along WOCE lines I1, I2, I3, I4, and the two Australian lines. The more saline Red Sea Water is distinguishable in stations located within 100 km of the African coast and in the core of the Agulhas Current south of I4 (Beal and Bryden, 1999). Lower oxygen concentrations are also found at these same stations than east of Madagascar (not shown). Harris (1972), Gordon (1986), and Beal et al. (2000), all showed that water in this region close to the coast with low oxygen and high salinity was derived from the Mozambique Channel and not from the Indian Ocean interior east of Madagascar.

Despite the large-scale evidence for southward flow, when data from individual cruises are considered the idea of a continuous MC transporting water from the southern Somali Basin through the Mozambique Channel to the Mozambique Basin finds less support. Clowes and Deacon (1935) speculated on the importance of remote forcing mechanisms (such as the strength of the monsoon winds) in determining intermediate and deep water mass composition and variability. Harris (1972) further reported that a front in both hydrographic properties and acceleration potential separates the inner and outer portions of the Agulhas Current and extends well into the Mozambique Channel. He stated that water outside the front, characterized by higher oxygen concentrations, is supplied by two main sources, from the SEC via the EMC and through recirculation from the Agulhas Return Current recycled west of the Madagascar Ridge. Waters shoreward of the front come south through the Mozambique Channel.

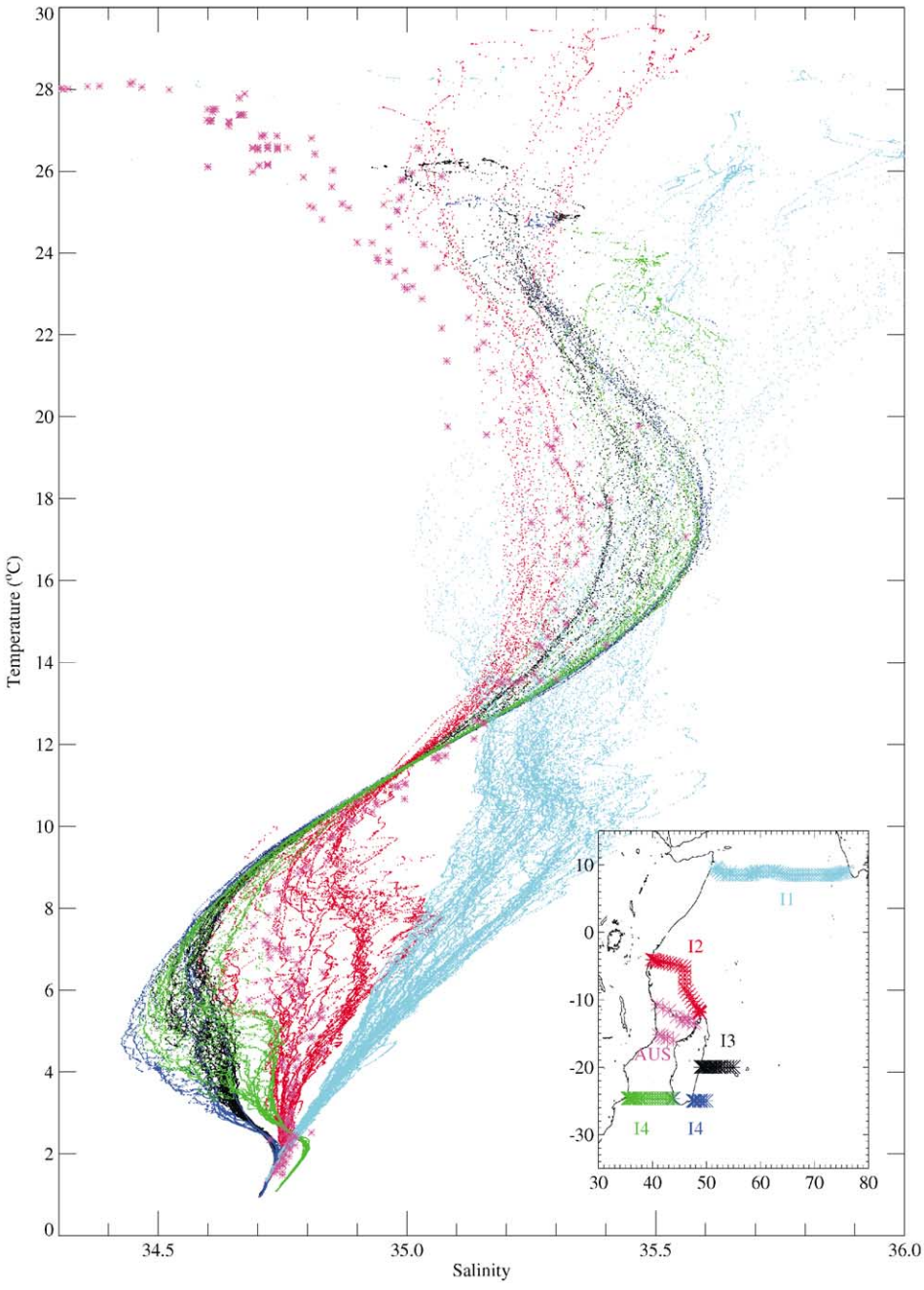

Fig. 3. Temperature-salinity relationships characteristic of intermediate water from WOCE Indian Ocean lines I1, I2, I3, I4, and I5W; see inset for station positions. Purple crosses show individual samples from the 1965 cruises; the remaining data are from CTD casts.

Lutjeharms (1976) showed that during the northeast monsoon (defined as November–April), low-salinity water of tropical origin was found on both sides of the southern part of the channel above about 120 m, and that it had clearly come from the north and not from east of Madagascar. While he also inferred southward flow through the channel at depths of 300–400 m, below this depth the flow appeared. The major source of the Agulhas Current then appeared to be the EMC negligible, which looped northwards west of Madagascar before turning south on the western side of the channel. Thus, according to Lutjeharms, the source of flow for the Agulhas Current seques from the MC near the surface, to a mixture of the MC and EMC in the thermocline, with the EMC being the only contributor at greater depths. This interpretation WOCE data is inconsistent with the modern.

Saetre and Jorge da Silva (1984) also doubted the continuous nature of the MC. They investigated the seasonal variability of the current based on six different hydrographic surveys taken during 1957–1964. While they showed from T/S analysis that north of about 23–25°S the channel is filled with water from the northern Indian Ocean, they found no evidence for a continuous extension of these waters into the Agulhas Current. Their analysis produced results similar to Harris (1972) suggesting that the general upper circulation pattern in the Mozambique Channel consists of three anticyclonic gyres covering the northern, central, and southern parts of the channel, each highly conditioned by the topography, and that the positions and even existence of the three gyres may vary considerably. During the winter the anticyclonic gyres in the northern and central regions may join to form an anticyclonic deep tongue that extends the central well into channel (at 20°S). (This would presumably give rise to the structure seen by Clowes and Deacon, 1935, as their *Discovery* data were taken in April/May of that year.) In summer, the two northern gyres may be separated by a cyclonic eddy at 16–18°S that blocks water attempting to cross the Davie Ridge from the north, and thus effectively interrupts southward MC flow. However, examination of their figures suggests that continuous flow through the channel is possible in winter, although considerable meandering is necessary.

Donguy and Piton (1991) showed in an analysis based on differences in pressure gauges measurements from each side of the channel that the meridional flow in the northern and southern Channel is in phase and contains a clear seasonal cycle. However, these measurements are confined to the upper 500 m and say nothing about the seasonality at depth.

4. Results

4.1. Hydrography

Given the importance of water mass structure and composition to the geostrophic calculations presented later, we describe first the main features of the hydrography and water masses, bearing in mind that a subject of the data are not contemporary and that the I2 and I4 data were taken in opposite seasons of the year. A companion analysis of the regional hydrography is underway by Donohue and Toole (in preparation).

Gordon et al. (1987) give an excellent account of the complex inter-relationships of the different water masses in the western Indian Ocean, as determined from T/S and T/O analysis, while Wyrtki (1971) provides a series of complementary seasonal property maps on depth and core layer surfaces. According to Wyrtki, austral summer sea-surface temperatures and salinities (January–February) north of Madagascar are in the range 28–29°C and 34.5–35.0, respectively. In winter (May–August) the sea-surface temperature drops to 25–27°C, while salinity increases to about 35.2. To the south, colder surface temperatures are observed: 24–25°C (summer) and 20–22°C (winter) at about 30°S, while salinities near this latitude are around 35.5–35.6. Somewhat lower salinities (35.2–35.3) are found in the southern portion of the Mozambique Channel close to the African coast, but there is otherwise little zonal variability. Below the surface, salinity increases in the subtropical waters south of 20°S compared to the northern tropical region, and differences in oxygen concentration also become more marked. These

changes are particularly obvious in the T/S plot (Fig. 3), where the low salinity of the Tropical Surface Water (TSW) contrasts with the higher salinity Subtropical Surface Water formed in the 25–35°S latitude band where evaporation exceeds precipitation.

Along I2, surface temperatures exceeded 29°C at the surface (Fig. 4), with low salinities (generally 35.1–35.3) characterizing the upper 300 m, particularly close to the northern tip of Madagascar. This is a clear signal of the influence on the SEC of TSW, which has a relatively low salinity because of the excess precipitation and because it contains Pacific water transported via the Indonesian throughflow. Along the western portion of I2, the surface salinity was above 35.4, particularly on the near-zoned portion of the section west of station 1231. On I4, surface salinities were much

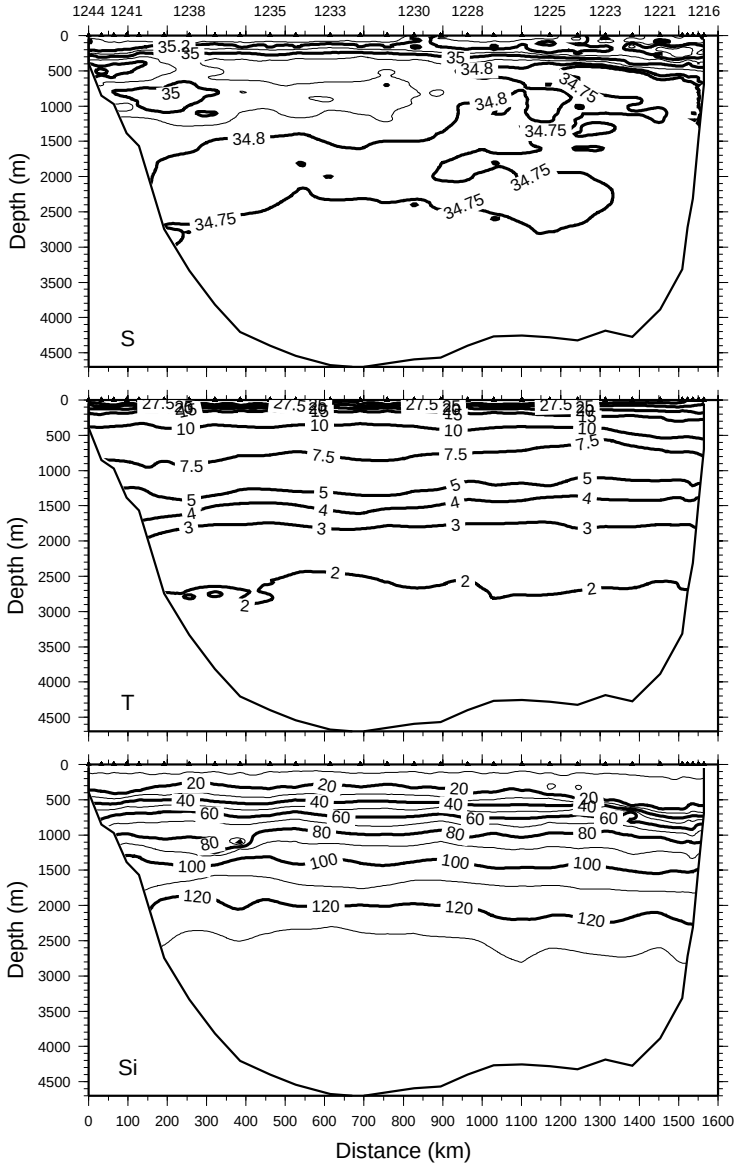

Fig. 4. Salinity (top), temperature (middle) and silicate (bottom) sections along WOCE section I2 between Africa and Madagascar.

higher, above 35.4 (Fig. 5), as expected from historical data. Along the two Australian lines, however, while the lower surface temperatures reflect the winter (May) sampling period, the extremely low salinities are puzzling. Water with salinity <35.0 was found across both lines in the upper 50 m. Although many rivers feed the Mozambique Channel from both Madagascar and Mozambique, they would not affect such a thick layer. It seems likely that during this period low salinity water from the SEC was rounding Cape Amber and pushing south through the Channel at the surface. This is very different from the WOCE period, when data suggest the 35.0 and 35.1 isohalines reached west only to about 75°E and 52°E, respectively (Gordon, 1997), or from October–November 1957 when surface salinities in the Channel were 35.2–35.3 (Menaché, 1963), but Wyrtki (1971) suggests that low-salinity water may be found farther west than this in all months.

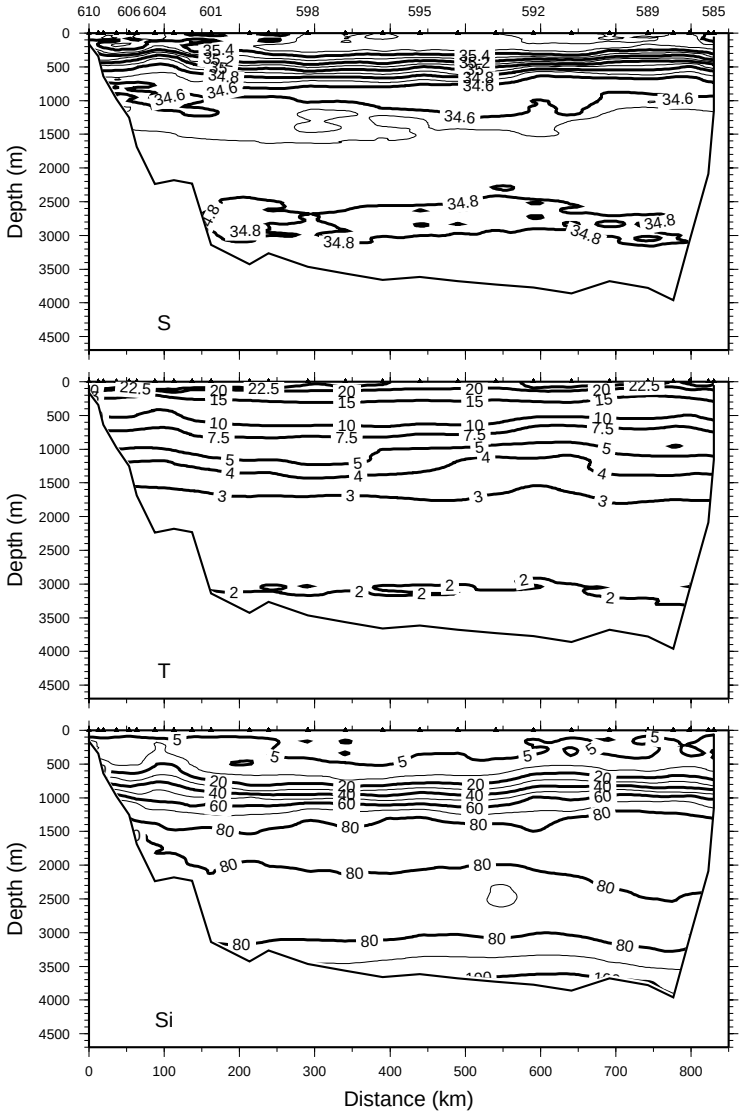

Fig. 5. Salinity (top), temperature (middle) and silicate (bottom) sections along WOCE section I4 between Africa and Madagascar.

Below the subtropical salinity maximum, the T/S relationship in the Southwest Indian Ocean becomes linear in the central water layer. The deviation from linearity varies, depending on whether the water in the 800–1400 m depth range comes from the north (Red Sea Water; RSW), or from the south (Antarctic Intermediate Water; AAIW). The former is produced by the sinking of warm overflow water in the Gulf of Aden, which produces a local intense salinity maximum and an associated oxygen minimum, visible in the I1 data at temperatures near 8–10°C (Fig. 3). Although the RSW salinity is reduced considerably by the time it reaches 10–20°S, it remains about 0.2–0.3 more saline than AAIW. In Fig. 3, the T/S data from the Australian lines show clearly that the water at this level was all from the north, with all but two samples having salinities of 34.7–34.8 below 600 m depth. AAIW, on the other hand, originates south of 40°S and therefore is a low-salinity water mass with relatively high oxygen concentrations, seen in Fig. 3 as the salinity minimum on I3 and I4 between 4–6°C.

The hydrography along the western part of I2 was dominated by the salinity signal, which distinguishes water originating north or south of the equator, particularly at mid-depth (500–1500 m), and the 34.8 isohaline forms a good indicator that separates the water in the east and west. Immediately north of Madagascar, this isohaline is found near 600 m. It shoaled gradually to the north, reaching 400 m depth near station 1223, and maintained this depth as far as station 1228 (7°30′S), where it plunged to below 1200 m. Between these two stations there is clearly interleaving with fresher water (Fig. 4), which shows the influence of AAIW that has moved north in the Indian Ocean interior, and then west to round Cape Amber.

The salinity along the northern portion of I2 is consistently above 34.9 in the 700–1300 m depth range, indicative of RSW its northern origin. A remarkable feature is seen at stations 1238–1240, where the salinity increases above 35.0. The T/S plot (Fig. 3) and the LADCP data (later) show clearly that this must be an eddy of Red Sea Water. How this anticyclonic eddy managed to cross the equator, or whether it formed in situ south of it, is beyond the scope of this paper; its origin is discussed elsewhere (Beal and Donohue, submitted).

Along I4 the temperature and salinity plots (Fig. 5) show a preponderence of water from the south. A salinity minimum (<34.6) stretches across the whole section at 800–1000 m depth, while water in the 2500–3000 m depth range shows a maximum (>34.8) derived from NADW. Below 1500 m on I2 salinities are almost constant at 34.7–34.8. Thus, any water with salinity <34.7 at these depths within the Channel must derive from the south. The T/S plot is essentially vertical in the 34.7–34.8 range for the data from the Australian stations with no hint of values below 34.7. This separation of water from north and south within the Channel agrees with the data from Clowes and Deacon (1935, see Fig. 2) and the limited deep data from Menaché (1963). Menaché found water fresher than 34.7 only south of 22°S.

The shape of the isohalines along I4 in the depth range 1000–1500 m suggests, in fact, that water of northern origin is still found at this latitude, particularly on the western side of the Channel, as shown by the green data points in Fig. 3 at temperatures between 3–5°C. The T/S plot for stations on I4 west of the island (green) clearly differs from stations east of the island (dark blue in Fig. 3), where no such high-salinity (>34.7) water is found. This plot clearly indicates the southward movement of water through the Mozambique Channel that contributes to the inshore portion of the Agulhas Current (see also Beal et al., 2000 and the data in Menaché, 1963). These data also contradict the auguments in Lutjeharms (1976).

Other notable features are also visible in Fig. 5. Two cyclonic eddies can be seen at stations 591–592 and 603–604, shown by the doming of the isotherms, isohalines, and the silicate isopleths above 1000 m. These eddies are also seen in the oxygen section (Fig. 6) and the LADCP data (Fig. 7). The third feature is an apparent northward flow along the bottom at stations 601–605, seen in the upward-sloping isotherms, oxygen and silicate isopleths and in the LADCP data. This is likely the northern extension of the deep undercurrent found further south in the Agulhas region by Beal and Bryden (1999).

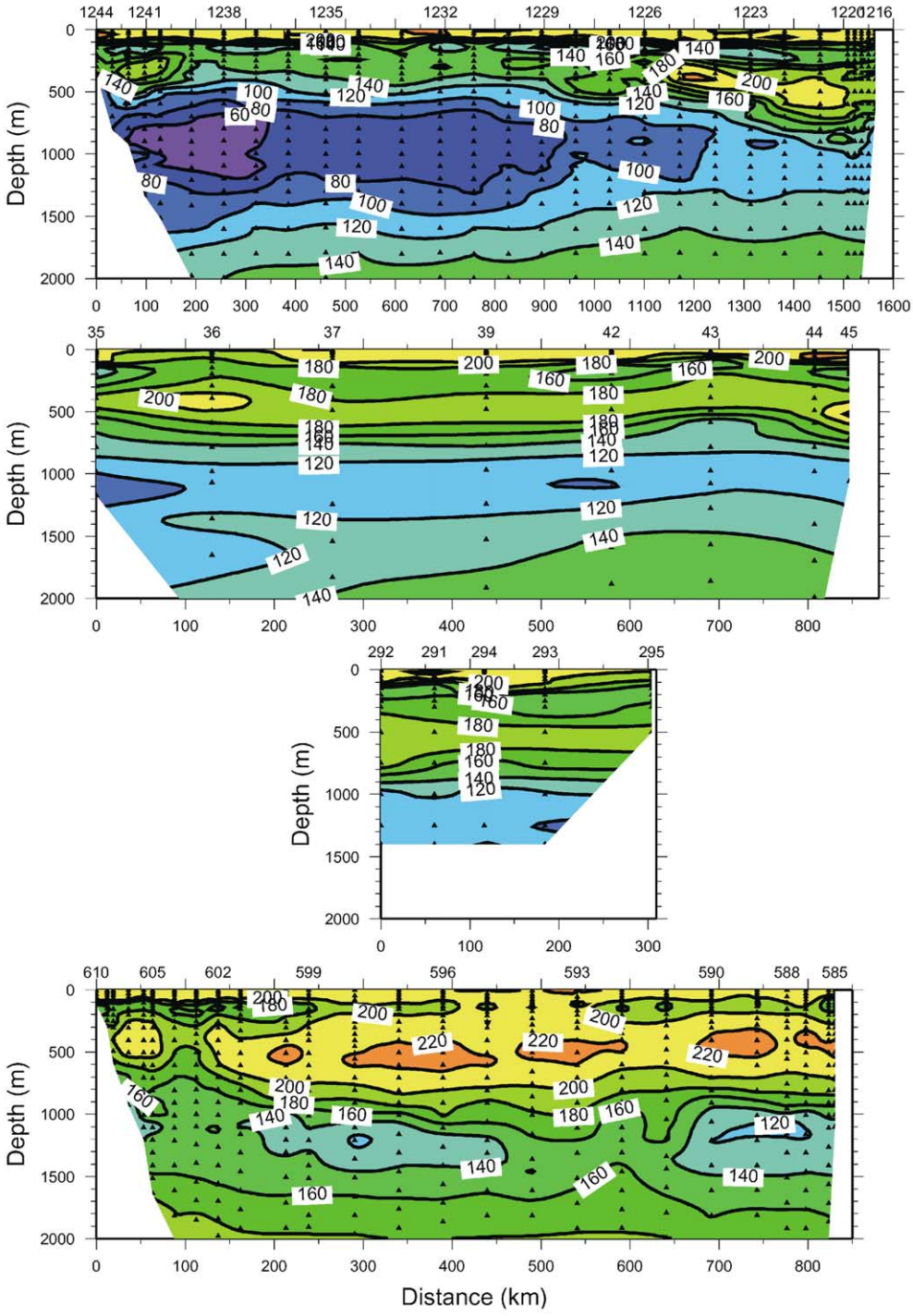

Fig. 6. Dissolved oxygen concentration (μmol kg^{-1}) observed on four vertical sections spanning the Mozambique Channel or its source waters: (upper) WHP I2, (two middle) 12°S and 15°S 1965 Australian sections, (lower) WHP I4. Station locations are shown in Fig. 1.

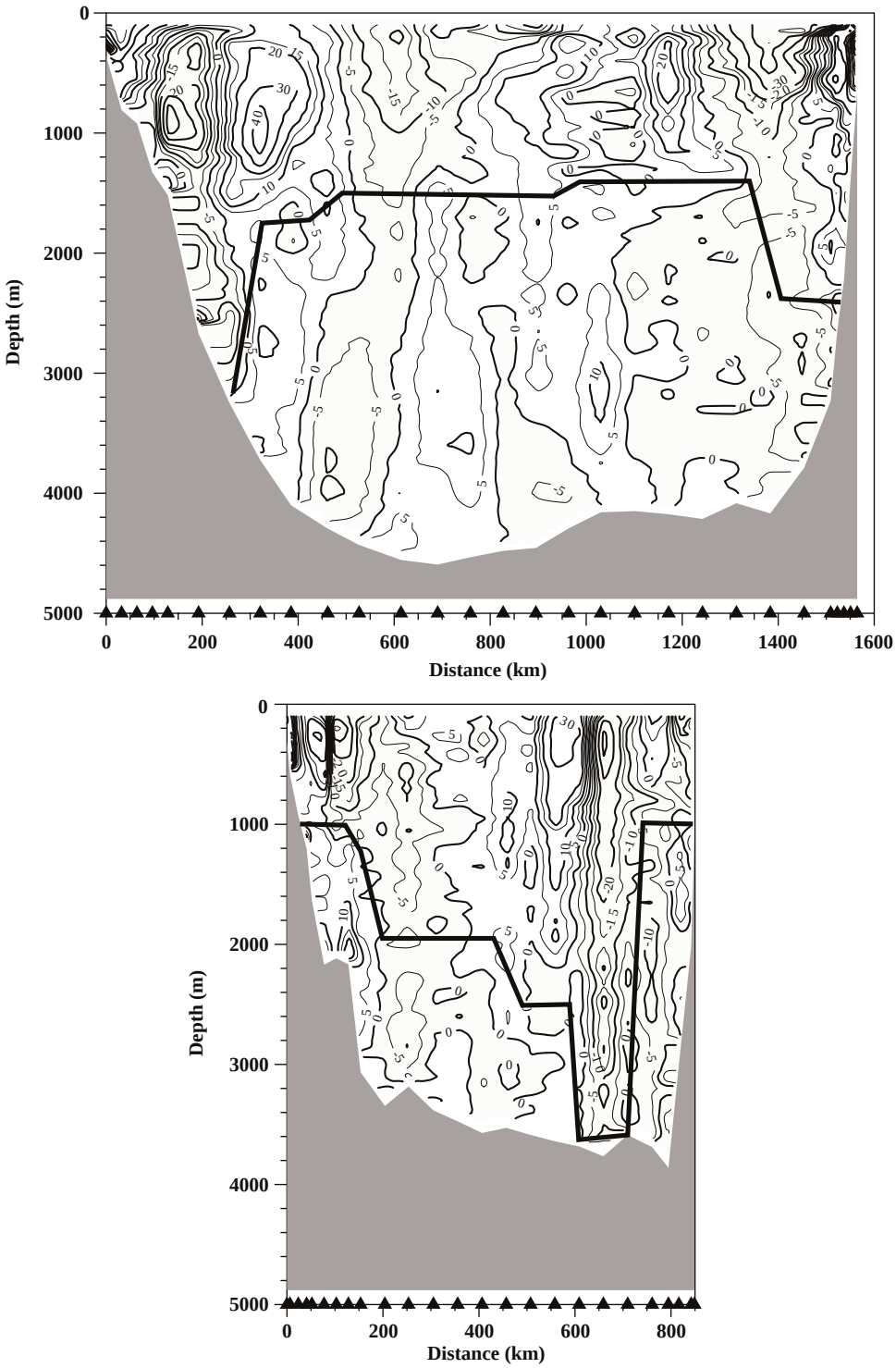

Fig. 7. Cross-track (essentially meridional) ADCP current component ($cm\,s^{-1}$) along WHP line I2 (top) and I4 (bottom). Southward currents are shaded; east is at the right side of the page and west on the left. Station positions are represented by triangles and their geographical locations are shown in Fig. 1. The heavy dashed lines show the reference depths used to calculate the geostrophic transports.

The deep waters also are separated by whether they possess a northern or southern origin. The deep basins of the northern Indian Ocean are filled with North Indian Deep Water (NIDW), which shows a uniform decrease in both temperature and salinity with depth (Fig. 3, I1 data) and contains high silicate concentrations (Fig. 4). South of 20°S, however, the salinity and oxygen content below the intermediate water layer rise to maxima, while the dissolved silicate shows a local minimum in the North Atlantic Deep water (NADW) (Fig. 5). The reverse (lower oxygen and salinity but higher silicate) occurs in the bottom water, which is mainly Circumpolar Deep Water (CDW). The separation of the NIDW and CDW is shown clearly in Fig. 3.

Additional evidence for southward flow is shown in the oxygen data (Fig. 6). A high-oxygen core of South Indian Central Water (SICW), with oxygen values $>200\,\mu mol\,kg^{-1}$, is seen at 500 m just north of Madagascar flowing west with the SEC; it is also seen continuing northward near the African coast in the Zanzibar Current, where values have been reduced to somewhat $>180\,\mu mol\,kg^{-1}$. This high-oxygen layer must continue to flow west across the northern end of the Channel, likely north of the Comores near 10°S, as there is no sign of an oxygen maximum between stations 1228 and 1239 (Fig. 6a). At 12°S (second panel of Fig. 6) the maximum forms a band across the Mozambique Channel characterized by values above $180\,\mu mol\,kg^{-1}$. Concentrations above $200\,\mu mol\,kg^{-1}$ are found at two stations-one at the eastern end of the line and one about 100 km east of the western end. The band of oxygen $>180\,\mu mol\,kg^{-1}$ is still present across the width of the Channel at 15°S (third panel) although no values reached $200\,\mu mol\,kg^{-1}$. However, one should bear in mind the coarse station resolution in these two Australian sections, which may have missed sampling the relatively narrow oxygen maximum.

This distribution of dissolved oxygen at the maximum is thus consistent with the idea of flow into the Mozambique Channel from the north via the SEC and southward flow principally near the western boundary. Wyrtki (1971) also showed that nutrient concentration levels at the core of this oxygen maximum are significantly higher in the Mozambique Channel, particularly on its western side, than east or south of Madagascar, supporting our hypothesis of southward flow. However, this simple picture is complicated along I4 (lowest panel) where all stations east of 602 showed oxygen concentrations higher than farther north. While such differences might be caused by seasonal effects, this seems unlikely at this depth, and we believe it is caused by the input and/or recirculation in the southern part of the Channel of water with higher oxygen concentrations from south and east of Madagascar. In this regard, the T/S plot (Fig. 3) shows clearly that the water between 9–13°C along I4 is very different from that further north in the Channel, having the properties found further south near the Subtropical Convergence Zone (Gordon, 1986; Gordon et al., 1987).

Fig. 6 also shows clearly the southward deepening and increase in oxygen concentration at the level of the RSW intermediate oxygen minimum. Note that this pattern is not well resolved in the 15°S section, due to poor station and bottle spacing. The lowest RSW oxygen concentrations along the northern two lines were found adjacent to the African coast. Minimum values increased from $<60\,\mu mol\,kg^{-1}$ near 900 m on I2 to nearly $140\,\mu mol\,kg^{-1}$ near 1100 m on I4. This again indicates southward spreading through the channel, with erosion of the oxygen-minimum layer from above by waters of southern origin containing higher oxygen concentrations. Similarly, Fig. 3 shows highest salinities west of the island at the depth of the Red Sea water. Beal et al. (2000) also present data showing low oxygen concentrations in this layer.

All the above suggest that there is a continuous southward flow of water through the Mozambique Channel. Much of the water originates in the northern Indian Ocean, but the oxygen data also suggest southward movement of water, originally from the southern hemisphere gyre, that rounds the northern tip of Madagascar. In the southern Mozambique Channel, however, additional water of southern origin occurs as a result of mixing and recirculation south of Madagascar. There is no

evidence, however, of this recirculating water flowing northwards across the Davie Ridge.

4.2. Direct Velocity Observations

LADCP transport calculations provide independent estimates of flow based on directly observed absolute velocities. The LADCP velocity observations from the I2 and I4 lines are shown in Fig. 7. For each section the cross-track velocity component is plotted. The most striking features on both sections are the large-scale (greater than 100 km) velocity structures which have a significant barotropic (depth-averaged) component, particularly along I4 (e.g., near 38°E and 42°E). In addition there are more intense eddy features in the upper 2000 meters. The eddies are often associated with the large-scale barotropic structures. The following provides a brief discussion of the dominant features seen in these sections and of the transport calculations based on them.

Northwest of Cape Amber we see the SEC flowing to the west between 9–11.8°S. The current is intensified in the upper 1200 meters and has a significant barotropic component. Near Cape Amber an intense small eddy extends to 1000 meters with eastward flow just offshore of the cape. The eddy may be associated with the separation of the SEC flow from the north end of Madagascar. Just north of the SEC an eastward jet was observed with a subsurface maximum near 600 meters. Along the east-west segment, we observe a banded structure of alternating northward and southward currents. Adjacent to the African coast, the northward flowing East African Coastal Current was sampled, extending to a depth of 800 meters. To its east a remarkable subsurface eddy was observed with peak velocities near 900 meters. The T/S data show that this is clearly composed of Red Sea Water, with salinity >35.0 (see Figs. 3 and 4). The eddy diameter at this depth is about 250 km. Near 5.2°S, 46°E the flow pattern suggests open ocean eddy features.

At the western end of the I4 section, southward flow was observed close to the coast between the surface and 600 meters (Fig. 7, bottom). This flow may be part of a small eddy with its northward limb just to the east, and/or may be a jet associated with the surface-intensified Mozambique Current. Over the depth range 1000–3000 meters, close to the continental slope, the flow is to the north within 200 km of the African coast. This may be a northward extension of the Agulhas Undercurrent seen further south by Beal and Bryden (1999). Further along the I4 section, the dominant features are two eddy structures centered near 36.4°E and 41.7°E. These are surface-intensified with peak velocities near 200–400 meters. The western eddy, near 36.4°E, disappears below 1000 m but is associated with further southward flow whose structure below 1000 meters appears tilted strongly towards the east. At 42°E (700 km in Fig. 7) there is also a large barotropic component to the south associated with the southward branch of the upper-ocean eddy. The interpretation of the observed velocity in terms of eddy features rather than semi-permanent meridional flows is consistent with the observed property distributions along the section. Increased near-bottom flow is found in both southward features below 2500 m depth.

Transport calculation based on these LADCP data suggest that the transport across I2 is 17 +/− 9 Sv towards the north/east and of 9 +/− 13 Sv to the north and east for the whole water column. In contrast, flow across I4 is estimated at 27 +/− 24 Sv to the south above 2500 m, with a full depth flow of 43 Sv to the south. The large uncertainties result from possible small biases in the velocities which can add up to large transports over large areas, tidal effects, and transient barotropic phenomena. The LADCP data are simply difficult to use for transport estimates. For instance, below 2500 m, where the still of the Davie Ridge blocks the Mozambique Channel, the LADCP data suggest large southward transport at I2 and even larger southward transport at I4. However, the error bars are so large than none of the transports for any depth range are significantly different from zero. However, the LADCP data do suggest the possible importance of barotropic flow in the mean, with near-surface currents often extending to the bottom. This potential barotropic component suggests caution in relying too heavily on geostrophic transport estimates either.

4.3. Transport estimates

Geostrophic velocities and volume transports across the WOCE I2 and I4 lines were estimated. The lowered ADCP data (Fig. 7) were used to estimate an initial level of no motion, and the levels for each station were adjusted to give zero volume, mass and salt transport below 2500 m depth. This depth corresponds to the sill depth within the Mozambique Channel. The chosen reference levels for each station pair are shown in Fig. 7. Along I2, the reference level was taken as either the bottom (at either end of the line) or close to 1500 m; along I4, the level sloped upwards from station 590 towards the west. Volume transport was estimated by integrating the relative velocity between two stations from the surface to the reference level and multiplying by the area represented by that velocity. The resulting southward net transports are 29.1 Sv for I2 and 5.9 Sv for I4. The difference in the transports below 2500 m from zero was <0.1 Sv across both lines, with $<0.5\%$ for the mass and salt fluxes.

The cumulative transport across the lines is given in Fig. 8. Across I2, the northward coastal jet and the eddy at the western end of the line are clearly visible, with a stronger northward transport occurring on the eastern side of the eddy between 300 and 500 km from the coast. The rest of the section generally exhibits flow to the south and west, with regions of concentrated transport about 700 and 1400 km from the African coast. (The bend in the I2 section at station 1232 coincides with the 700 km point.) These correspond to regions of strongly barotropic southward and westward flow in the ADCP data (Fig. 7). Along I4, the northward flow in the eddy at the western end of the section is more than compensated by the region of deep reaching southward flow further to the east, between 200 and 300 km, while the intense eddy centered at 600 km has little effect on the net transport.

The vertical distribution of flow, based on these geostrophic estimates, is shown in Fig. 9. The transports have been calculated in 250-m bands from the surface to the bottom. Transport across I2 shows intense shear in the upper 500 m, with flow below 1300 m varying from zero by only about 1–1.5 Sv for any band, except at the bottom where flow below 4250 m reaches about 2.5 Sv. This net transport to the north of bottom water well below the still depth of the Davie Ridge is probably indicative of either errors in our choice of reference level or temporal variability sampled by the quasi-synoptic section. Across I4, the transport is again surface-intensified, with almost all the net transport occurring above 1200 m depth.

The large difference between the two volume transport estimates is surprising. However, the two sections were made during opposite monsoons (January and June for I2 and I4, respectively), so the wind stress across the region was undoubtedly very different during the two cruises. The presence of eddies also seems likely to affect the calculation; De Ruijter et al. (2002) suggest that the passage of an eddy through the Channel is equivalent to a net transport of 15 Sv southwards. Such eddies are clearly visible on both lines in the upper 1500 m (Fig. 7). Regions of barotropic flow are also present on both lines. We suspect that these are transient features, which will therefore provide additional variability.

Ekman transports are a small fraction of the total transports at I2 and I4. The Ekman transports across I2 estimated from a monthly wind stress climatology (Hellerman and Rosenstein, 1983) ranged from -3 Sv in January (the month that I2 was occupied) through 2 Sv in July with a mean of -0.2 Sv. For I4, the seasonal cycle was much smaller and ranged from -0.9 Sv in March to -0.5 Sv in June (the month that I4 was occupied), with a mean of -0.7 Sv.

The new net transport estimates through the Mozambique Channel from I2 and I4 lie within the range of historical and model estimates (Table 1). We have included calculations for I2 and I4 using constant reference levels of 1000 and 2000 m, although these do not produce zero net flow below the 2500 m Davie Ridge still depth, to give some idea of the sensitivity of transports to reference level estimates and for ease of comparison to historical estimates, which often used the 1000 m level. Historical transport estimates based on hydrography range from 5 Sv northward to 26 Sv southward depending on reference level. We

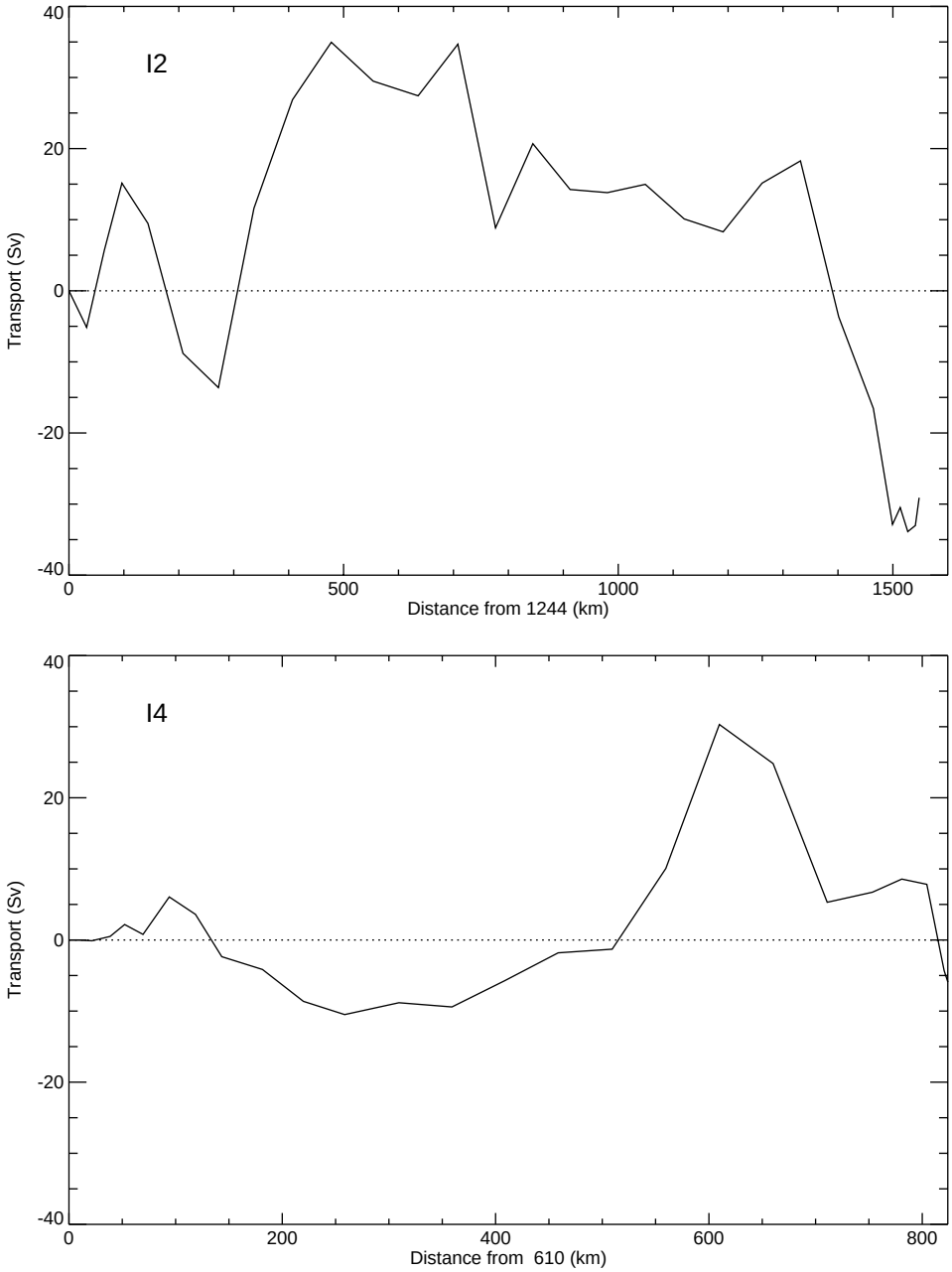

Fig. 8. Cumulative transport (Sv) across I2 and I4 using the reference depths shown in Fig. 7.

believe 1000 m to be a poor choice for reference level and that the resulting variability may only reflect the seasonal changes of shear or shorter time-scale eddy variability in the upper 1000 m. Further, the large variability of geostrophic transport in the upper 1000 m has lead to creative interpretations of transport estimates during different seasons. Some of these estimates also suffer

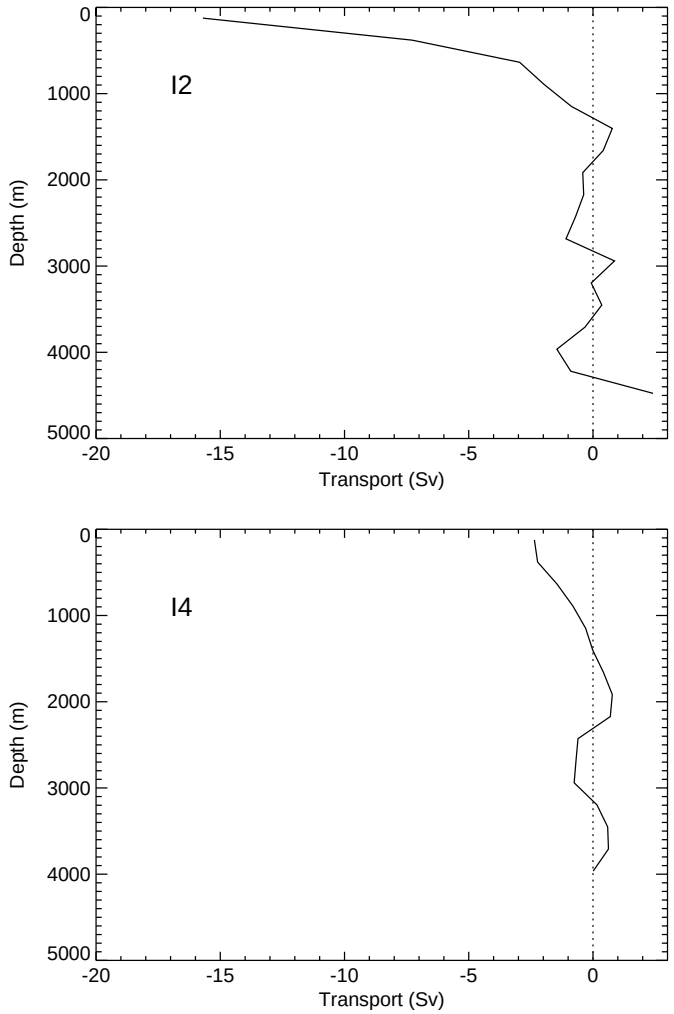

Fig. 9. Vertical distribution of mean zonal transport across lines I2 ands I4 based on 250-m deep segments. Note that in the transport estimate across I2, negative values indicate both southward and westward movement because of the shape of the line.

from poor coverage in key areas adjacent to the African and Madagascar continental slope and shelves, thus omitting any contribution due to western intensification. This is most noticeable in Zahn's estimate of 6 Sv north at 26°S. The picture is further complicated because some of the currents move onto the continental shelves where geostrophic flow is hard to estimate.

While our "best" I2 and I4 geostrophic transport estimates (those with variable reference levels) do differ significantly from each other, they have two advantages over most of the historical estimates. First, they are made using closely-spaced hydrographic sections extending to the bottom. Second, the reference levels used are guided by information from direct velocity (LADCP) measurements. The addition of these two more modern sections suggests that determining the mean transport through the passage will require a data set of relatively dense spatial and temporal resolution.

Results from models based on hydrographic data show variable MC volume transports. Using an inverse model, Fu (1986) estimated the

Table 1
Historical and model estimates of volume transport in the Mozambique Channel

Transport (Sv)	Reference (m)	Data source	Reference
20–26 South	1000	Hydrography	Duncan (1970)
10 South	2500	Hydrography	Harris (1972)
15 South[a]	600	Hydrography	Nehring et al. (1984)
6 South (15°S)	1000	Hydrography	Zahn (1984)
5 North (26°S)[a]	1000	Hydrography	Zahn (1984)
19.4 South (Feb/Mar)	500	Hydrography	Donguy and Piton (1991)
9.4 South (Mar)	500	Hydrography	Donguy and Piton (1991)
14 South (July)	500	Hydrography	Donguy and Piton (1991)
5 South	1000	Hydrography	Stramma and Lutjeharms (1997)
15 South[b]	1500	Lowered ADCP	De Ruijter et al. (2002)
6 South	1500	Inverse model	Fu (1986)
0.3 North	2000	Inverse model	MacDonald and Wunsch (1996)
16 North to 35 south	Full depth	LANL POP model	Maltrud et al. (1998)
10 North to 20 south	Full depth	3.5 layer model	Ji and Luther (1998)
3 North to 22 south	Full depth	Kiel MOM	Biastoch and Krauss (1999)
14 ± 6 South	Full depth	Inverse model	Ganachaud and Wunsch (2000)
15 ± 6 South	2500 m	Inverse model	Ganachaud et al. (2000)
14 ± 9 South	Full depth	Inverse model	Ganachaud et al. (2000)
29.1 South	Variable	Hydrography	WOCE I2
21.5 South	1000	Hydrography	WOCE I2
23.3 South	2000	Hydrography	WOCE I2
5.9 South	Variable	Hydrography	WOCE I4
4.5 South	1000	Hydrography	WOCE I4
19.0 South	2000	Hydrography	WOCE I4

[a] Did not extend to coasts.
[b] Rectified transport in a Mozambique Channel ring.

southward transport to be 6 Sv relative to 1500 m and that the net mass flux below 2000 m was "very small", which appears incorrect based on lowered ADCP data presented in the next section. MacDonald and Wunsch (1996) reported a global estimate of ocean circulation and heat transport based on the application of inverse techniques to some 23 hydrographic sections, principally from the 1980s, but some from the 1960s (e.g., the two May 1965 Australian sections mentioned above). The resulting meridional velocity fields were quite complicated with considerable flow both northward and southward (MacDonald, 1998); net volume transports from the model were 0.2 ± 1.4 Sv at 12°S and 0.3 ± 1.6 Sv at 15°S. However, a global inversion of WOCE data estimates net flow through the Mozambique Passage at 14 ± 9 Sv at I2 starting with a bottom reference level and 15 ± 6 Sv at I4 starting with a 2500 m reference level (Ganachaud et al., 2000).

Prognastic models have also been used to investigate flow in the region. Biastoch and Krauss (1999) and Biastoch et al. (1999) used a MOM-model of the Indian Ocean with 1/3° resolution and 29 levels (AGAPE). While their mean flow through the channel was only about 10 Sv south, the results show considerable seasonal variability with near zero flows in February–April and maximum southward flows near 20 Sv in July–August. Unfortunately, no error estimates on the flow are given in either of these papers, which are the first to use a fine-resolution model of the region, neither is there any information on eddy activity. As these authors used climatological values for surface wind stress, it is likely that the

instantaneous flow from observations will differ considerably from such model results.

4.4. Floats

To date, other than the two ADCP lines already discussed and a more recent transect illustrated in De Ruijter et al. (2002), there have been no direct measurements of subsurface flow through the Mozambique Channel. However, the ALACE floats released during WOCE cruises provide a series of independent estimates of the flow field at about 800–900 m depth. Davis (1991, 1998) has discussed the use of float data to obtain current velocities, and advocated using each monthly record of displacement as an independent measurement of velocity. Thus, if one has a considerable number of records from a given area, estimates of the mean flows can be made. We have analyzed trajectories of the 55 floats that entered this portion of the Indian Ocean (35–55°E, 5–30°S) between May 1995 and December 1999. These gave a total of 835 records over the four and a half years. Because of the small number of floats in the region at any given time, we have combined the data into four sub-regions: the eastern approach to Madagascar between 15–25°S, the northeast quadrant around Cape Amber to 49°E, the northern portion of the Channel extending as far south as the narrows, and the southern portion of the Channel. The speed distributions (ignoring direction) for the northern and southern portions of the Channel are given in Table 2, along with the E–W and N–S velocity components. We also have separated out the boundary current regimes, defined somewhat arbitrarily as being within two degrees of longitude of the coast of Africa. Speeds and velocity components for these regions are listed separately.

The mean speeds in both regions are close to 6–7 cm s^{-1} (Table 2) apart from within the two boundary currents, the East African Coastal Current (EACC) and the Agulhas Current. Speeds in the boundary currents are about twice the areal mean and are again nearly equal, however, the number of trajectories in the EACC was very small. The range in speeds in all areas however, is large, and individual monthly movement can be large whether or not the float is in a boundary current, as can be seen in the individual float tracks in Fig. 10. Some floats (not shown here) entered the region from the east, spent considerable time (up to two years or more) around the northern part of Madagascar, and then exited to the east again. Others, such as the six tracks shown in Fig. 10, passed southwards through the Channel more or less directly.

When direction is taken into account the mean E–W and N–S velocity components drop considerably (Table 2), while the variability, as shown by the standard deviations, rises by about 50% compared to that for the speeds. We believe that this shows the importance of the highly variable eddy field in the region, even at depths of 800 m or more. The eddies themselves likely move with translation speeds of about 5–7 cm s^{-1}, as found

Table 2
Float speed/velocity statistics

	N. Moz. Chan		S. Moz Chan		EACC	Moz/Agulhas
Mean speed (cm s^{-1})	7.24	6.79	10.20	7.51	15.17	16.75
Std. dev.	4.53	4.02	6.92	4.37	5.87	7.52
Std. error	0.24	0.22	0.60	0.44	2.22	1.24
N	345	326	131	98	7	37
E–W mean (cm s^{-1})	−0.32	−0.18	−2.90	−0.89	−2.26	−6.46
Std. dev.	5.76	5.61	6.97	5.62	6.91	7.18
Std. error	0.31	0.31	0.61	0.57	2.61	1.18
N–S mean (cm s^{-1})	−0.55	-0.58	−3.52	−0.66	11.29	−12.44
Std. dev.	6.28	5.52	9.03	6.57	9.99	9.55
Std. error	0.34	0.31	0.79	0.66	3.78	1.57

For columns 2–5, the first number in each pair shows the statistics for all data, the second for data not in western boundary currents.

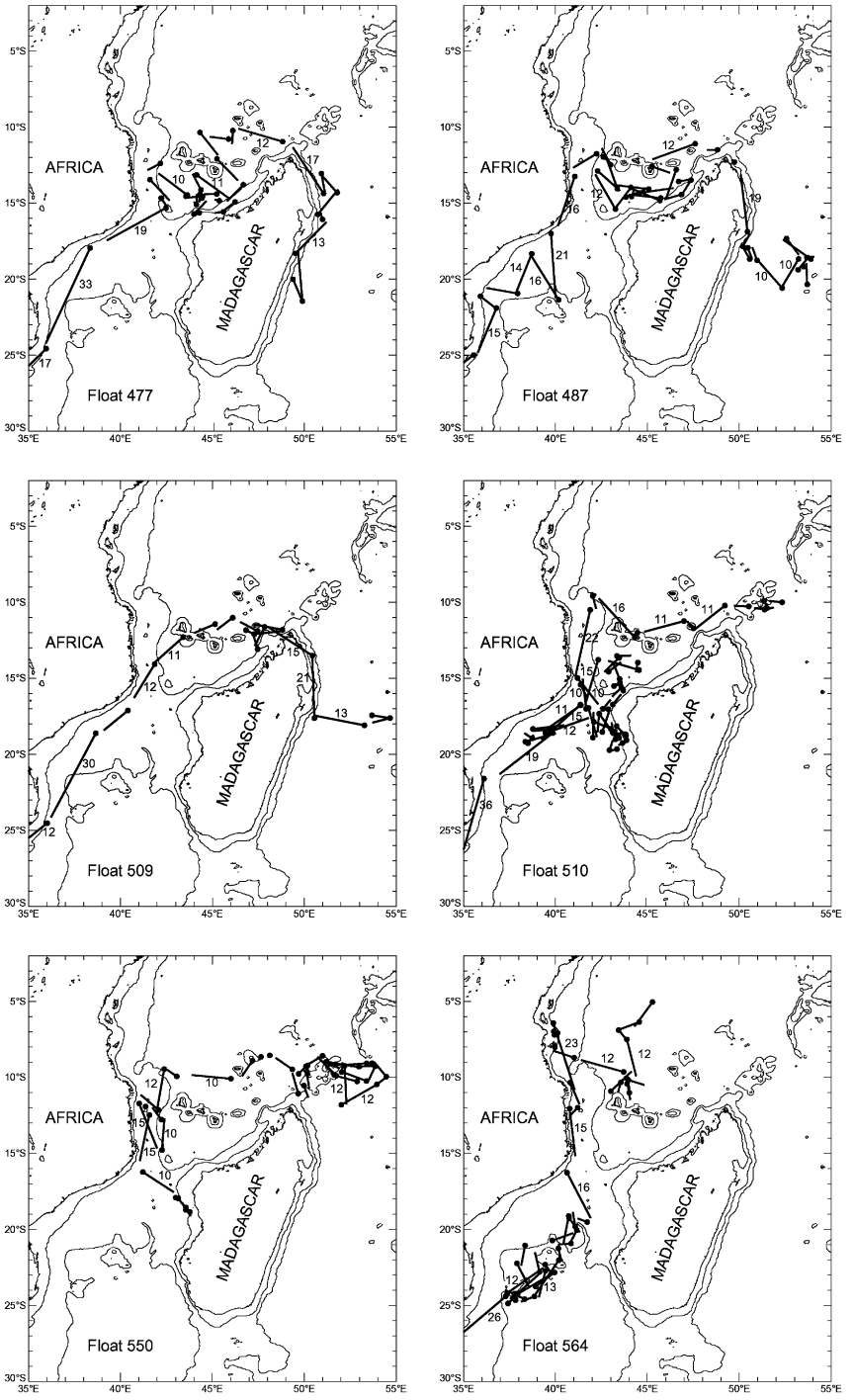

Fig. 10. ALACE float trajectories in the southwest Indian Ocean showing six floats that moved southward through the Mozambique Channel at depths between 700 and 900 m. Float numbers are indicated. Dots represent the beginning location of each float cycle. Average float speed is depicted at the midpoint between the start and end point of each 25 day float cycle for speeds of 10 cm s^{-1} or greater. The 1000-m and 3000-m isobaths are shown. Data cover the period June 1995 through December 1999.

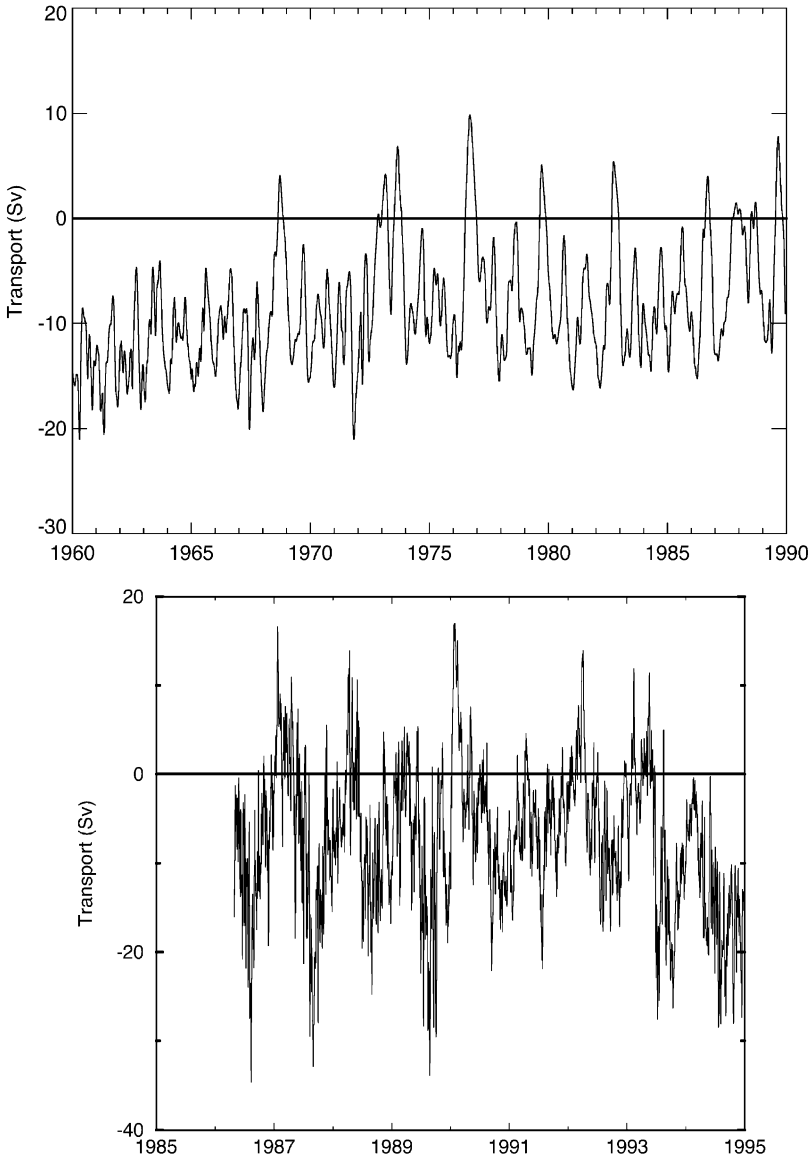

Fig. 11. (upper) Transport through the Mozambique Channel from the model of Ji and Luther (1999). (lower) Transport through the Mozambique Channel from the LANL 1/6° POP model run by Maltrud et al. (1998). Dates are at mid years.

further west in the Benguela region (Olson and Evans, 1986), but their radial velocities can be considerably higher. De Ruijter et al. (2002) have shown that surface drifters can make several circuits of an eddy in the southern Mozambique Channel within one month, and if an ALACE float is caught in a deep eddy, it would be expected to behave similarly, as found for continually tracked RAFOS floats in the Cape Basin west of Africa (Richardson et al., 2000).

ALACE floats cannot be tracked except when they are at the surface, so there is no information

on their movements during the 25 days they spend submerged between each position fix. Capture of the float by a deep eddy may well explain the strange apparent motion of float 487 near 20°S; examination of the TOPEX-derived sea-surface height data available from Dr. R. Leben (University of Colorado) shows the presence of a large anticyclonic eddy near 20°S, 40°E at this time. Thus, the velocities given in Table 2 are likely underestimates. However, even without taking this into account, the net flow in both the northern and southern portions of the Mozambique Channel is significantly to the southwest at mid-depth, especially when the western boundary regions are not excluded from the velocity estimates.

Although considerable eddy activity (both anticyclonic and cyclonic) is to be seen in the individual float tracks north of Madagascar and in the northern half of the Mozambique Channel, the six floats that moved south over the Davie Ridge into the northern Mozambique Basin all crossed at the western end of the ridge. These six trajectories are shown separately in the six panels of Fig. 8. Average float speed is indicated at the midpoint between start and end locations of each 25-day cycle, where the velocities were $10\,cm\,s^{-1}$ or larger. Float 564 was the only float of the 55 examined that showed southward movement between 5°S and 12°S close to the African coast. All floats showed complex patterns of movement and low velocities suggesting interaction with eddies north of the saddle and around the Comoro Islands between 10°S and 15°S; floats 477 and 487 passed south of the Comoro Islands, the remainder moving past the islands to the north. Floats 510 and 564 also showed eddy motion in the southern part of the channel. However, of these six floats, all but 550 eventually reached the western boundary in a jet and were entrained into the Agulhas Current. Floats 477 and 509 had average speeds of $\sim 30\,cm\,s^{-1}$ in the boundary current on the western side of the channel. Floats other than 550 showed velocities of $15–30\,cm\,s^{-1}$ along the western boundary. The data from float 550 end in December 1999 with the float in the eastern part of the channel.

Floats approaching Madagascar from the east showed a bifurcation in their path near 20°S. Some floats moved south within the EMC, others north in a similar fashion to that found by Shenoi et al. (1999) and Lutjeharms et al. (2000) for surface drifters and ships' drift estimates. Typical paths of three of the northward-moving floats (477, 487, 509) are shown in Fig. 10. Two of the southward-moving floats passed south of Madagascar, moved west, and ultimately reached the African coast; a third appears to have retroflected south and east near 43°E. Both anticyclonic and cyclonic eddy activity was found east of Madagascar, particularly at the northern end of the island.

The float trajectories suggest that most of the intermediate water coming through the Channel comes from east of Madagascar. As such, they seem at odds with the results from hydrography, particularly the oxygen data, which suggest that the water between 500 and 2000 m comes from the north. It should be noted, however, that only four of the floats were released northwest of Madagascar between 5°S and 15°S, and one of these survived only two months before running aground on the Comores. Floats released equatorward of 5°S were entrained in the zonal equatorial current system. We believe that there is certainly flow into the Channel from both north and east of the island, but that the strong stirring, particularly around the Comoro Islands, serves to entrain northern water properties into waters of the interior of the South Indian subtropical gyre making up the SEC that passes into the northern Mozambique Channel north of Cape Amber.

4.5. Satellite data variability

Eddies are ubiquitous in the region; Heywood and Somayajulu (1997) analyzed ERS-1 sea-surface height data for the period October 1992–December 1993 and showed that both the rms sea level anomalies and the eddy kinetic energy (EKE) are much higher in the Mozambique Channel than east of Madagascar. The EKE data show enhanced values southward from the SEC through the Channel. Wunsch and Stammer (1995) have shown similar results from TOPEX data; their Plate 2 shows a band of high variability in

sea-surface elevation extending from the Agulhas into the Mozambique Channel.

TOPEX/POSEIDON sea-surface height differences between 44°E and 36°E averaged between 20° S and 25°S (Jochem Marotzke, pers. commun.) and show prominent, low-frequency fluctuations with excursions up to 80 cm. This analysis is based on a $2^\circ \times 2^\circ$ gridded product constructed by Stammer and Wunsch (1994). The spectrum (not shown) shows a peak at about 80 d, significant at 95%. Although the absolute value of the time mean should be ignored because of geoid uncertainties, for a linear change of pressure gradient between the sea surface and a 1000-m reference level, the sea-surface height would correspond to transport excursions of up to 80 Sv. This assumption of a linear change between 0–1000 m probably leads to a high estimate, since much of the variability is likely contained within the thermocline. However, the model results in Fig. 11 suggest temporal transport variability of 30–50 Sv through the channel over periods of several months.

The drifter data of Molinari et al. (1990) and Shenoi et al. (1999) show that the SEC has its maximum velocity in austral winter and spring (May–September). During this time the wind-stress curl south of the SEC shows a strong gradient, in contrast to the austral summer. Heywood and Somayajulu (1997), in their analysis of ERS-1 data, stated:

> The zero wind stress curl is located slightly further north in winter than summer, but this does not appear to influence the location of the maximum in eddy kinetic energy, which extends, if anything, further south in winter than summer. The important influence is that in winter (the southwest monsoon season) the wind speed in the Trades is greater over the whole of the South Equatorial Current (5–20°S). This leads to higher eddy kinetic energy, both indirectly by forcing the SEC faster which then is more inclined to baroclinic instabilities, and directly by generating eddies through fluctuating wind stress curl.

Whether this increase in EKE translates into increased transport in the MC, either baroclinic or barotropic, remains unknown. If we believe the model results cited above, however, then the models are in agreement with the idea of strengthened southward flow in winter.

4.6. Model results

We have compared our hydrography-based transport estimates with those of a series of models in Table 1. Time series of volume transport through the Mozambique Channel based on two different model outputs are shown in Fig. 11. The lower panel shows meridional transport at 17°S from the Los Alamos National Laboratory (LANL) (POP) model driven by European Community mean wind field (ECMWF) 3-day averaged winds and the Barnier heat flux for the period 1986–1995 (Maltrud et al., 1998; shown courtesy of Albert Semtner). The LANL POP model run has 1/6° resolution and is a 20-level primitive equation model. The upper panel shows the transport time series for 1960–1990 from a 1/12°, 3.5-layer Indian Ocean model (Ji and Luther, 1999), which simulates flow in the upper 800–1000 m of the water column using the first 3 baroclinic modes (the barotropic mode is not admitted) and is driven by the monthly mean winds and surface thermal fields of Jones et al. (1995). Dates in both panels are at mid years.

Both models show an average long-term transport through the Channel of about 10 Sv south. Superimposed on this is considerable low-frequency variability with a total range of about 40 Sv (10–15 Sv northwards to 25 Sv southward), which is similar to transport fluctuations derived from altimeter sea-surface height differences. Spectral analysis (not shown) showed energy peaks at periods of about 170 days in the POP model and 180 and 360 days in the 3.5-layer model. We also note that the seasonal variability may be partially barotropic for the POP model, but must be wholly baroclinic by construction for the 3.5-layer model. The apparent trend to lower southward transports seen in the 3.5-layer model probably results from a similar trend in the wind stress and wind stress curl in the Jones et al. (1995) surface fields.

Much of the transport variability in these models is seasonal. In January (summer), the MC is at its weakest, while in August (winter) it is strongest. Transports range from 22 Sv to the south during the southwest monsoon to as much as 10 Sv to the north during the northeast monsoon. Such transport values are consistent with those from the AGAPE model (Biastoch and Krauss, 1999; Biastoch et al., 1999), as reported earlier, although the unquantified error bars on the seasonal flows are large (A. Biastoch, pers. commun.). The annual variability in this model is about 20 Sv, with energetic eddy activity in both seasons. Similar data obtained from the 1/4° Ocean Circulation and Climate Advanced Modeling Project (OCCAM) (David Webb and Andrew Coward, pers. commun.) also show a continuous stream of eddies, almost all anticyclonic, exiting the southern end of the Mozambique Channel along the western boundary.

By construction, inverse models using closely-spaced data show more consistent southward flow. Results of Ganachaud and Wunsch (2000) and Ganachaud et al. (2000), using WOCE data, suggest flow of around 15 Sv southward through the Mozambique Channel. Such models provide an integrated best-fit solution for the region studied, but cannot estimate the seasonal variability in the same way as forward models. These data can be contrasted with the results of MacDonald and Wunsch (1996) which used older, more widely-spaced data sets (including the two Australian sections).

Our transports, calculated from geostrophy, are out of phase with such a seasonal variation—the low flow (5.9 Sv) southwards across I4 was found in June, while the high flow (29.1 Sv) across I2 was found in January. If, however, the majority of the flow is carried by eddies, as suggested by De Ruijter et al. (2002), with four eddies per year and each eddy equivalent to 15 Sv, then the apparent mismatch may be reversed depending on when the eddies are formed and when the stations were sampled. These results show the difficulty of obtaining representative transports from single sections, especially in regions of high variability.

5. Discussion

The data shown here clearly support the idea of southward flow through the Mozambique Channel into the Agulhas Current formation region. This flow has a large variable component that may be barotropic and seasonal (as suggested by the LADCP data; satellite data and model results discussed above) or due to random eddy variability (as suggested also by De Ruijter et al., 2002). Since, however, no time-series studies have yet been published from the narrowest part of the Channel, it is not possible to distinguish between the two possibilities. The vertical (shear) and horizontal distribution of the flow also are not known with any certainty, although the available hydrographic snapshots lead to the belief that the southward flow is frequently intensified along the African coast and that the flow is strongly sheared in the upper few hundred meters. In situ measurements of this variability are needed to help determine the interocean transport of heat and freshwater and establish the global balances of these parameters, as well as the relative importance of the "warm-water route" (Gordon, 1986), which passes through the Channel, to the global ocean circulation.

Despite the presence of the EMC there is clearly a net anticyclonic flow around the island that contributes the oxygen maximum seen moving south through the Channel in our data. This is counteracted by northward flow east of the island, primarily at the eastern edge of the subtropical gyre in the layers attributable to SAMW, Central Water, and AAIW. These waters meet the SEC at the northern edge of the gyre, forcing them west and keeping them separate from the waters of northern Indian Ocean origin. The Mascarene Plateau at 5–20°S effectively blocks zonal transport below the upper few hundred meters. Thus, the southern waters come south again and can only continue to the northwest to round the northern tip of Madagascar once the flow bifurcates near 20°S.

There is likely also northward flow closer to Madagascar. Robbins and Toole (1997) estimated a net poleward transport above 2000 db across a zonal track near 32°S, finding interior

equatorward flow east of the Agulhas Current including in the Mozambique Basin. Fine (1993), using oxygen and CFC distributions, similarly showed that Antarctic Intermediate Water (AAIW) in this region has an equatorward meridional component, which is strongest near 60°E. This northward movement appears to be continuous throughout the Crozet and Madagascar Basins; additional data from the I3 (20°S) and I7C (24°S) WOCE lines between Madagascar and Mauritius (20°S, 58°E) show oxygen-rich water flowing north or northwest between 200 and 600 m depth, as do data from a 1985 cruise on the *Marion Dufresne* at 23°S (Swallow et al., 1988). Current-meter data from Swallow et al. (1988) also show weak northward geostrophic flow at distances > 100–150 km east of the island at this latitude.

Flow through the Mozambique Channel is almost certainly affected by remote forcing. For instance, the model results of Hirst and Godfrey (1994) suggest that a stronger Indonesian throughflow results in higher SSTs in the Agulhas region. How deep this surface layer penetrates, and whether any increased southward flow occurs west or east of Madagascar, remain open questions. However, a simple sensitivity study of the effect of varying the transport of the Indonesian throughflow in an inverse box model suggests little impact on transports in the Mozambique Channel region (MacDonald and Wunsch, 1998). Presumably, given the dependence of the EKE of the region on the strength of the south east trade winds (Heywood and Somayajulu, 1997), the interannual variability of the large-scale wind field in the southern Indian Ocean also will affect the strength of the MC.

6. Conclusions

In summary, the property distributions, transport estimates, and direct current measurements show the Mozambique Channel to have a complex and variable system of currents, which interact and mix at several depth levels. Historical estimates of volume transport through the channel based on hydrographic data range from 5 Sv northward to 26 Sv southward. We have estimated the volume transport through the Mozambique Channel using new hydrographic measurements obtained during WOCE legs I2 and I4 in the channel's northern and southern ends. We find southward transport above 2500 m of 29.1 and 5.9 Sv for I2 and I4, respectively.

Analysis of four vertical oxygen sections across different locations of the channel are consistent with southward spreading through the channel. Lower oxygen concentrations indicative of a northern hemisphere Red Sea Water source were found across the whole of the Channel as far south as the Narrows near 1000 m depth, and were intensified on the western side as least as far south as the Comoro Islands. Above this, a high-oxygen layer was found to round Cape Amber and fill the region south of the Comoros at a depth of about 500 m. Highest oxygen concentrations were found along the southernmost line, I4, indicating the contribution of waters transported south in the EMC and/or recirculated from further south in the Madagascar Basin.

Float trajectories indicate considerable eddy activity north and east of Madagascar and in the northern Mozambique Channel, as well as a highly variable speed regime. The float-based mean velocity within the Mozambique Channel is low, but to the south and west. The float trajectories indicate two possible pathways for water within the SEC east of Madagascar to join the Agulhas Current on Africa's south east coast. The SEC reaches the east coast of Madagascar near 20°S and splits. The northern route forms a northward flowing boundary current up the east coast and around Cape Amber, from where the water flows west around the Comoro Islands, then south along the African coast through the Mozambique Channel. The southern route moves south with the EMC and around the southern tip of Madagascar, then westward toward the African coast. The small number of observations precludes any conclusions on which route is more important. Similarly, we cannot say whether both occur continuously or whether any pulsing takes place which causes one route to predominate at different times.

Model results show considerable seasonal variability, but generally have long-term average

southward transport of about 10 Sv. As stated above, the data support the idea of southward flow through the Mozambique Channel, however, only a comprehensive measurement program that includes a time-series of direct measurements across the narrow, central portion of the Channel will ultimately determine the transport's variability and seasonality. Although the I2 and I4 lines are eddy-resolving, they are a considerable distance from the narrowest part of the channel and both are subject to the influence of eddies (as shown in Figs. 4 and 5) which may alias the transport signal. We await the results of the recent Dutch current-meter deployments across the Channel with interest. Future work on transport estimates through the Channel should also include the application of the Island Rule (Godfrey, 1989) to the Indian Ocean and comparing the resulting estimates to the estimates presented here.

Acknowledgements

Funding for W.D.N, P.C., and S.F.D was provided under NSF grants OCE-94-01590 and OCE-96-17985. Funding for P.H. and K.D. was provided under NSF grants OCE-98-18947 and OCE-94-13172. Funding for G.C.J. was provided by the NOAA Office of Global Programs and the NASA Physical Oceanography Program. I4 and I7C data were collected with support of NSF grants OCE-94-01343 (J. Toole) and OCE-94-13164 (J. Swift). We would like to thank two anonymous referees and the following people who contributed data and thoughtful comments to this paper: L. Beal, H. Bryden, R. Davis, E. Firing, R. Hetland, K. Heywood, R. Leben, M. Maltrud, J. Marotzke, A. MacDonald, J. McClean, and B. Semtner. Maps and some contouring were produced using the Generic Mapping Tools (GMT) software package (Wessel and Smith, 1995).

References

Beal, L.M., Bryden, H.L., 1999. The velocity and vorticity structure of the Agulhas Current at 32°S. Journal of Geophysical Research 104, 5151–5176.

Beal, L.M., Ffield, A., Gordon, A.L., 2000. Spreading of the Red Sea overflow waters in the Indian Ocean. Journal of Geophysical Research 105, 8549–8564.

Biastoch, A., Krauss, W., 1999. The role of mesoscale eddies in the source regions of the Agulhas Current. Journal of Physical Oceanography 29, 2303–2317.

Biastoch, A., Reason, C.J.C., Lutjeharms, J.R.E., Boebel, O., 1999. The importance of flow in the Mozambique Channel to seasonality in the greater Agulhas Current system. Geophysical Research Letters 26, 3321–3324.

Clowes, A.J., Deacon, G.E.R., 1935. The deep-water circulation of the Indian Ocean. Nature 136, 936–938.

Davis, R.E., 1991. Observing the general circulation with floats. Deep-Sea Research 38 (Suppl. 1), S531–S571.

Davis, R.E., 1998. Preliminary results from directly measuring mid-depth circulation in the tropical and south Pacific. Journal of Geophysical Research 103, 24619–24639.

Davis, R.E., Webb, D.C., Regier, L.A., Dufour, J., 1992. The autonomous Lagrangian circulation explorer (ALACE). Journal of Atmospheric and Oceanographic Technology 9, 264–285.

De Ruijter, W.P.M., Ridderinkhof, H., Lutjeharms, J.R.E., Schouten, M.W., Veth, C., 2002. Direct observations of flow in the Mozambique Channel. Geophysical Research Letters, in press.

Di Marco, S.F., Chapman, P., Nowlin Jr., W.D., 2000. Satellite observations of upwelling on the continental shelf south of Madagascar. Geophysical Research Letters 27, 3965–3968.

Donguy, J.-R., Piton, B., 1991. The Mozambique Channel revisited. Oceanologica Acta 14, 549–558.

Duncan, C.P., 1970. The Agulhas Current. Ph.D. Dissertation, University of Hawaii, 76pp.

Duncan, C.P., Schladow, S.G., 1981. World surface currents from ship's drift observations. International Hydrographic Review LVIII, 101–112.

Dushaw, B.D., Egbert, G.D., Worcester, P.F., Cornuelle, B.D., Howe, B.M., Metzger, K., 1997. A TOPEX/POSEIDON global tidal model (TPXO.2) and barotropic tidal currents determined from long-range acoustic transmissions. Progress in Oceanography 40, 337–367.

Egbert, G.D., Bennett, A.F., Foreman, M.G.G., 1994. TOPEX/POSEIDON tides estimated using a global inverse model. Journal of Geophysical Research 99, 24821–24852.

Fine, R.A., 1993. Circulation of Antarctic intermediate water of the South Indian Ocean. Deep-Sea Research I 40, 2021–2042.

Fisher, J., Visbeck, M., 1993. Deep velocity profiling with self-contained ADCPs. Journal of Atmospheric and Oceanographic Technology 10, 764–773.

Fu, L.L., 1986. Mass, heat, and freshwater fluxes in the South Indian Ocean. Journal of Physical Oceanography 16, 1683–1693.

Ganachaud, A., Wunsch, C., 2000. Improved estimates of global ocean circulation, heat transport and mixing from hydrographic data. Nature 408, 453–456.

Ganachaud, A., Wunsch, C., Marotzke, J., Toole, J., 2000. Meridional overturning and the large-scale circulation of

the Indian Ocean. Journal of Geophysical Research 105, 26117–26134.
Godfrey, J., 1989. A Sverdrup model of the depth-integrated flow for the world ocean allowing for island circulations. Geophysical Astrophysic Fluid Dynamics 43, 89–112.
Gordon, A.L., 1986. Interocean exchange of thermocline water. Journal of Geophysical Research 91, 5037–5046.
Gordon, A.L., 1997. Indonesian throughflow water streaks across the Indian Ocean. US WOCE Implementation Report 9, 9–11.
Gordon, A.L., McClean, J.L., 1999. Thermohaline stratification of the Indonesian seas: model and observation. Journal of Physical Oceanography 29, 198–216.
Gordon, A.l., Lutjeharms, J.R.E., Gründlingh, M.L., 1987. Stratification and circulation at the Agulhas retroflection. Deep-Sea Research 34, 565–599.
Gründlingh, M.L., 1985a. Features of the circulation in the Mozambique Basin in 1981. Journal of Marine Research 43, 779–792.
Gründlingh, M.L., 1985b. Occurrences of Red Sea water in the southwestern Indian Ocean. Journal of Physical Oceanography 15, 207–212.
Gründlingh, M.L., 1987. Cyclogenesis in the Mozambique Ridge Current. Deep-Sea Research 34, 89–103.
Gründlingh, M.L., 1989. Two contra-rotating eddies of the Mozambique Ridge Current. Deep-Sea Research 36, 149–153.
Gründlingh, M.L., 1993. On the winter flow in the southern Mozambique Channel. Deep-Sea Research I 40, 409–418.
Gründlingh, M.L., Carter, R.A., Stanton, R.C., 1991. Circulation and water properties of the southwest Indian Ocean, spring 1987. Progress in Oceanography 28, 305–342.
Hacker, P., Firing, E., Wilson, W.D., Molinari, R., 1996. Direct observations of the current structure east of the Bahamas. Geophysical Research Letters 23, 1127–1130.
Harris, T.F.W., 1972. Sources of the Agulhas Current in the spring of 1964. Deep-Sea Research 19, 633–650.
Hellerman, S., Rosenstein, M., 1983. Normal monthly wind stress over the World Ocean with error estimates. Journal of Physical Oceanography 13, 1093–1104.
Heywood, K.J., Somayajulu, Y.K., 1997. Eddy activity in the South Indian Ocean from ERS-1 altimetry. Proceedings of the Third ERS Symposium on Space in the Service of our Environment. Florence, March 1997 (ESA SP-414), pp. 1479–1483.
Hirst, A.C., Godfrey, J.S., 1994. The response to a sudden change in Indonesian throughflow in a global ocean GCM. Journal of Physical Oceanography 23, 1895–1910.
Ji, Z., Luther, M.E., 1999. Circulation and heat budget of the Indian Ocean in a numerical model. OMPL Report #99-06-1, University of South Florida, St. Petersburg, FL., 142pp.
Jones, C.S., Leger, D.M., O'Brien, J.J., 1995. Variability in surface fluxes over the Indian Ocean: 1960–1990. The Global Atmosphere and Ocean System 3, 249–272.
Lutjeharms, J.R.E., 1972. A quantitative assessment of year-to-year variability in water movement in the south-west Indian Ocean. Nature 239, 59–60.
Lutjeharms, J.R.E., 1976. The Agulhas Current system during the northeast monsoon season. Journal of Physical Oceanography 6, 665–670.
Lutjeharms, J.R.E., 1988a. On the role of the East Madagascar Current as a source of the Agulhas Current. South African Journal of Science 84, 236–238.
Lutjeharms, J.R.E., 1988b. Remote sensing corroboration of the retroflection of the East Madagascar Current. Deep-Sea Research 35, 2045–2050.
Lutjeharms, J.R.E., Machu, E., 2000. An upwelling cell inshore of the East Madagascar Current. Deep-Sea Research I 47, 2405–2411.
Lutjeharms, J.R.E., Wedepohl, P.M., Meeuwis, J.M., 2000. On the surface drift of the East Madagascar and Mozambique Currents. South African Journal of Science 96, 141–147.
MacDonald, A.M., 1998. The global ocean circulation: a hydrographic estimate and regional analysis. Progress in Oceanography 41, 281–382.
MacDonald, A.M., Wunsch, C., 1996. A global estimate of ocean circulation and heat fluxes. Nature 382, 436–439.
Maltrud, M.E., Smith, R.D., Semtner, A.J., Malone, R.C., 1998. Global eddy-resolving ocean simulations driven by 1984–1994 atmospheric fields: Part I, mean circulation and variability. Journal of Geophysical Research 103, 30825–30854.
Menaché, M., 1963. Premier Campagne Océanographique du "Commandant Robert Giraud" dans le canal de Mozambique, 11 Octobre–28 Novembre 1957. Cahiers Océanographiques XV, 224–249 (in French).
Molinari, R.L., Olson, D., Reverdin, G., 1990. Surface current distribution in the tropical Indian Ocean derived from compilations of surface buoy trajectories. Journal of Geophysical Research 95, 7217–7238.
Müller, T.J., Holfort, J., Delahoyde, F., Williams, R., 1994. Improving NBIS Mk III measurements. In: WOCE Operations Manual, Part 3.1.3., WHP Operations and Methods, WOCE Report 68/91, as revised November 1994.
Nehring, D., Arl, G., Bublitz, G., Gohs, L., Gosselck, F., Hagen, E., Kaiser, W., Kijhner, E., Michelchen, N., Postel, L., Saetre, R., Schemainda, R., Siegel, H., Silva, P., Wolf, G., 1984. The oceanological conditions in the western part of the Mozambique Channel in February–March 1980. Geodatätisch Geophysikalische Veroffentlichungen 4(39), 163 pp.
Olson, D.B., Evans, R.H., 1986. Rings of the Agulhas. Deep-Sea Research 33A, 27–42.
Richardson, P.L., Garzoli, S.L., Duncombe Rae, C.M., Fratantoni, D.M., Goni, G.J., 2000. Float trajectories at 750 m in the Benguela Current (KAPEX). Eos 81 (48) (Suppl.), F716 (abstract).
Robbins, P.E., Toole, J., 1997. The dissolved silica budget as a constraint on the meridional overturning circulation of the Indian Ocean. Deep-Sea Research I 44, 879–906.
Saetre, R., Jorge da Silva, A., 1984. The circulation of the Mozambique Channel. Deep-Sea Research 31, 485–508.
Saetre, R., 1985. Surface currents in the Mozambique Channel. Deep-Sea Research 32, 1457–1467.

Schott, F., Fieux, M., Kindle, J., Swallow, J., Zantopp, R., 1988. Boundary currents east and north of Madagascar. 2. Direct measurements and model comparisons. Journal of Geophysical Research 93, 4963–4974.

Send, U., 1994. Accuracy of current profile measurements. Effect of tropical and midlatitude internal waves. Journal of Geophysical Research 99, 16229–16236.

Shenoi, S.S.C., Saji, P.K., Almeida, A.M., 1999. Near-surface circulation and kinetic energy in the tropical Indian Ocean derived from Lagrangian drifters. Journal of Marine Research 57, 885–907.

Stammer, D., Wunsch, C., 1994. Preliminary assessment of the accuracy and precision of TOPEX/POSEIDON altimeter data with respect to the large-scale ocean circulation. Journal of Geophysical Research 99, 22584–22604.

Stramma, L., Lutjeharms, J.R.E., 1997. The flow field of the subtropical gyre of the South Indian Ocean. Journal of Geophysical Research 102, 5513–5530.

Swallow, J., Fieux, M., Schott, F., 1988. Boundary currents east and north of Madagascar. 1. Geostrophic currents and transports. Journal of Geophysical Research 93, 4951–4962.

Tchernia, P., 1980. The Indian Ocean. In: Descriptive Regional Oceanography. Pergamon Marine Series 3, 171–215.

Tomczak, M., Godfrey, J.S., 1994. Regional Oceanography: An Introduction. Pergamon, Oxford, 422pp.

Unesco, 1988. The acquisition, calibration and analysis of CTD data. A report of SCOR Working Group 51. Unesco Technical Papers in Marine Science, 54, 92pp.

Wessel, P., Smith, W.H.F., 1995. New version of the generic mapping tools release. EOS Transactions of AGU 76, 329.

WOCE, 1994. WOCE Operations Manual, Part 3.1.3., WHP Operations and Methods, WOCE Report 68/91, as revised November 1994.

Wunsch, C., Stammer, D., 1995. The global frequency-wavenumber spectrum of oceanic variability estimated from TOPEX/POSEIDON altimetric measurements. Journal of Geophysical Research 100, 24895–24910.

Wyrtki, K., 1971. Oceanographic Atlas of the International Indian Ocean Expedition, National Science Foundation, 531pp.

Zahn, W., 1984. Eine Abshutzung des Volumentransportes im Kanal von Mozambique wehrend des Zeitraumes Oktober–November 1957. Beitrage zum Meereskunde, Berlin 51, 67–74 (In German).